Integral cross sections for the electron-impact excitation of the $b\ ^1\Pi_u$, $c_3\ ^1\Pi_u$, $o_3\ ^1\Pi_u$, $b'\ ^1\Sigma_u^+$, $c_4'\ ^1\Sigma_u^+$, $G\ ^3\Pi_u$, and $F\ ^3\Pi_u$ states of N_2

Charles P. Malone,[1,2] Paul V. Johnson,[1] Xianming Liu,[3] Bahar Ajdari,[2] Isik Kanik,[1] and Murtadha A. Khakoo[2]

[1]*Jet Propulsion Laboratory, California Institute of Technology, 4800 Oak Grove Drive, Pasadena, California 91109, USA*

[2]*Department of Physics, California State University Fullerton, Fullerton, California 92831, USA*

[3]*Planetary and Space Science Division, Space Environment Technologies, 1676 Palisades Drive, Pacific Palisades, California 90272, USA*

(Received 5 April 2012; published 18 June 2012)

Integral cross sections for electron-impact excitation out of the ground-state level $X\ ^1\Sigma_g^+(v''=0)$ to the $b\ ^1\Pi_u$, $c_3\ ^1\Pi_u$, $o_3\ ^1\Pi_u$, $b'\ ^1\Sigma_u^+$, $c_4'\ ^1\Sigma_u^+$, $G\ ^3\Pi_u$, and $F\ ^3\Pi_u$ electronic states in N_2 are reported at incident energies ranging between 17.5 and 100 eV. We also provide excitation cross sections using emission-based excitation shape functions and optical oscillator strengths. These cross-section results are of great importance to planetary atmospheric modeling of the emissions observed in Earth's atmosphere as well as those of Titan and Triton, the largest moons of Saturn and Neptune, respectively. Critical comparisons of the present cross sections with previous values are presented in an effort to provide improved cross sections for electron excitation of this fundamental molecule's important transitions.

DOI: 10.1103/PhysRevA.85.062704 PACS number(s): 34.80.Gs, 34.80.Ht, 34.50.Gb, 33.70.Ca

I. INTRODUCTION

Molecular nitrogen is the primary atmospheric constituent of the Earth (78%), Titan (94%), and Triton (99.9%). Interaction of these atmospheres with the plasma of the solar wind and either the intrinsic (Earth) magnetic field or that of their respective parent bodies (Saturn and Neptune for Titan and Triton, respectively), as well as with direct solar photoionization, ensures an abundant supply of low-energy electrons through primary ionizing events. These secondary electrons are very effective in many of the relevant collision processes because both the excitation cross sections and the electron energy distributions peak in the same energy range. Collisions between such secondary electrons and neutral N_2 molecules result in emissions that provide an important diagnostic probe for understanding the ionospheric energy balance and the effects of space weather extending downward through the thermosphere, into the mesosphere. Ongoing measurements of Titan by the Cassini Ultraviolet Imaging Spectrograph (UVIS), as well as upcoming measurements of Pluto (which is expected to have an N_2 dominated atmosphere) by the New Horizons spacecraft, make interpretation of N_2 emission particularly timely [1–4]. However, in order to properly model the dynamics of these environments based on observed emissions, accurate $e^- + N_2$ collision parameters need to be made available [5–8].

We previously determined integral cross sections (ICSs) for electron-impact excitation of the $A\ ^3\Sigma_u^+$, $B\ ^3\Pi_g$, $W\ ^3\Delta_u$, $B'\ ^3\Sigma_u^-$, $a'\ ^1\Sigma_u^-$, $a\ ^1\Pi_g$, $w\ ^1\Delta_u$, and $C\ ^3\Pi_u$ states from the $X\ ^1\Sigma_g^+$ $(v''=0)$ ground-state level of N_2 (see Johnson *et al.* [9]). These ICSs were derived from the differential cross sections (DCSs) measured by Khakoo *et al.* [10] using electron energy-loss (EEL) spectroscopy. Recently, we improved our $C\ ^3\Pi_u$ state DCSs [11] (and subsequently our $C\ ^3\Pi_u$ state ICSs [12]) by extending the EEL coverage to include all vibronic contributions. This differed from Ref. [10] where only excitation to the $v'=0$ level of the $C\ ^3\Pi_u$ state was directly measured and Franck-Condon factors (FCFs) were used to estimate the contribution of the unmeasured vibronic transitions (i.e., excitation of the $v'>0$ levels) to the total $C\ ^3\Pi_u$ state excitation cross section. (The work also included DCSs and ICSs for the $E\ ^3\Sigma_g^+$ and $a''\ ^1\Sigma_g^+$ states [11–13].) While, in some cases, significant disagreements were observed between our results and those of previous measurements (e.g., Refs. [14–16]), recent *ab initio* theoretical studies [17–19] and EEL measurements [20] show significantly improved agreement with our results. Importantly, we also note the recent Lyman-Birge-Hopfield (LBH) emission-based $a\ ^1\Pi_g$ work of Young *et al.* [21]: After an extensive series of measurements designed to rule out any possible systematic or statistical errors in the experimental apparatus and methodology, it was concluded that the previously seminal emission-based $a\ ^1\Pi_g$ state excitation cross section of Ajello and Shemansky [22] was not reproducible and should be supplanted. In support of this assessment, we note the excellent agreement between the shape of the Young *et al.* [21] relative excitation shape function and the $a\ ^1\Pi_g$ state ICSs of Ref. [9]. In addition, this more recent [21] emission-based cross section now provides more consistent results from the SEE (Solar Extreme ultraviolet Experiment) and GUVI (Global Ultra-Violet Imager) instruments on the TIMED (Thermosphere Ionosphere Mesosphere Energetics and Dynamics) spacecraft [23], which further demonstrates converging agreement among $e^- + N_2$ excitation cross sections and is very encouraging. Furthermore, our recent EEL work [11,24] also demonstrated non-Franck-Condon behavior below approximately 50 eV for excitation of the $C\ ^3\Pi_u$ state [25,26]. ICSs for excitation of individual vibrational levels of the $C\ ^3\Pi_u$ state [12] show remarkable agreement with renormalized [12,27] emission-based measurements [28].

Molecular nitrogen is essentially transparent to solar radiation over a large spectral range from the infrared (IR) to the far ultraviolet (FUV), except for weak LBH absorption. Transitions to singlet *ungerade* states cause N_2 to be a strong absorber in the extreme ultraviolet (EUV) spectral range, whereby the present work is of enhanced importance. [Recently, EUV emissions from photon excitation of N_2 have been measured [29–33] (and references therein).] The present ICSs for electron-impact excitation out of the ground-state level $X\ ^1\Sigma_g^+(v''=0)$ to the $b\ ^1\Pi_u$, $c_3\ ^1\Pi_u$, $o_3\ ^1\Pi_u$, $b'\ ^1\Sigma_u^+$,

$c_4'\ ^1\Sigma_u^+$, $G\ ^3\Pi_u$, and $F\ ^3\Pi_u$ electronic states in N_2 were obtained at incident energies ranging between 17.5 and 100 eV. The vibrational (v') coverage of the excited electronic states was a function of the unfolded EEL range (∼12–13.82 eV) of Khakoo *et al.* [34] from whose DCSs the present ICSs were derived. Further, since many rovibrational levels of these states are predissociative, their respective excitation and emission cross sections are important parameters for understanding the [N]/[N_2] ratio in the thermosphere of nitrogen-dominated atmospheres.

Of the higher-lying states considered in the present work, five are singlet *ungerade* states that are connected to the $X\ ^1\Sigma_g^+$ ground state (which has a closed-shell configuration: $(1\sigma_g)^2(1\sigma_u)^2(2\sigma_g)^2(2\sigma_u)^2(1\pi_u)^4(3\sigma_g)^2$ [35]) via dipole-allowed transitions. Among these singlet *ungerade* states are the $b\ ^1\Pi_u$ and $b'\ ^1\Sigma_u^+$ valence states and the $c_4'\ ^1\Sigma_u^+$ Rydberg state (i.e., the first member, $n = 3$, of the $np\sigma_u$ Rydberg series converging to the $X\ ^2\Sigma_g^+$ state of N_2^+) that, via radiative decay to the $X\ ^1\Sigma_g^+$ ground state, give rise to the Birge-Hopfield I, II, and Carroll-Yoshino bands, respectively. These N_2 band systems are observed in the atmospheres of Earth, Titan, and Triton. The $3p\pi_u\ c_3\ ^1\Pi_u$ Rydberg state (also converging to the $X\ ^2\Sigma_g^+$ state of N_2^+) and $3s\sigma_g\ o_3\ ^1\Pi_u$ Rydberg state (converging to the $A\ ^2\Pi_u$ state of N_2^+) give rise to the Worley-Jenkins and Worley series of Rydberg bands, respectively. However, emissions from the $c_3\ ^1\Pi_u$ and $o_3\ ^1\Pi_u$ states are not readily observed since they are strongly predissociated with the yield approaching 100% [2,36–39]. Therefore, the present direct excitation (i.e., EEL) approach is superior to standard (spontaneous) emission-based measurements for determining excitation cross sections for these states. Stated explicitly, optical emission is too weak to be used for excitation function and cross-section measurements, leaving EEL measurements as the only practical approach. Furthermore, direct energy-loss-based measurements of $e^- + N_2$ provide constraints on high-resolution emission plus predissociation determination procedures, such as our joint experimental and theoretical [coupled-channel Schrödinger equation (CSE) model] work [7], concerning these higher-lying Rydberg-valence states of N_2.

II. DIRECT ELECTRON-IMPACT EXCITATION CROSS SECTIONS

Although electron collision processes involving N_2 have been extensively studied (e.g., Refs. [16,40–43]), there remains a critical and substantial gap in the experimental database of direct electron-impact excitation cross-section data. The only previous measurement for electron impact (direct excitation) ICSs of the "complete" set of higher-lying states covered in the present work was published roughly 35 years ago. Specifically, Chutjian *et al.* [44] published DCSs and ICSs for the $b\ ^1\Pi_u$, $c_3\ ^1\Pi_u$, $o_3\ ^1\Pi_u$, $b'\ ^1\Sigma_u^+$, $c_4'\ ^1\Sigma_u^+$, $G\ ^3\Pi_u$, and $F\ ^3\Pi_u$ states, along with several "unidentified" metastable features, at electron-impact energies (E_0) of 40 and 60 eV. This work was later renormalized by Trajmar *et al.* [16] using updated elastic electron scattering cross sections. (Note: Continued use of the original Chutjian *et al.* [44] and the companion Cartwright *et al.* [15,45] data still occurs in the literature for comparisons and in modeling work. However, this use is incorrect as these data are supplanted by the revised data of Trajmar *et al.* [16].) Additional DCS and ICS data was obtained by Trajmar and co-workers (i.e., Ratliff *et al.* [46]) for excitation of the $b\ ^1\Pi_u$ state at E_0 values of 60 and 100 eV. The overall gap in the available data at low electron-impact energies is of particular concern. Not only are the excitation cross sections for these states significant below 40 eV, but so are the electron number densities in upper atmospheric plasmas (e.g., Ref. [47]), which are responsible for exciting these transitions in these natural environments. Therefore, in terms of the energy dynamics in planetary atmospheres containing N_2, as well as for N_2 plasmas in general, *direct* measurements for some of the most important *excitation* cross sections for the higher-lying states of N_2 are needed.

Apart from this deficiency concerning the availability of low impact-energy ICS data for the high-lying states of N_2, a concern also arises due to the poorly constrained shape of the ICSs of Trajmar *et al.* [16] and Ratliff *et al.* [46], particularly for the $b\ ^1\Pi_u$, $c_3\ ^1\Pi_u$, $o_3\ ^1\Pi_u$, $b'\ ^1\Sigma_u^+$, and $c_4'\ ^1\Sigma_u^+$ states. The two previous direct-excitation experimental ICS data sets were each obtained at only two E_0 values: Trajmar *et al.* [16] at 40 and 60 eV, and Ratliff *et al.* [46] at 60 and 100 eV. Such sparse impact energy coverage is insufficient to describe and constrain models of atmospheric emissions, let alone *ab initio* theoretical predictions of these excitation processes, which remain essentially absent from the literature. The only published *ab initio* calculation we are aware of with sophistication, beyond semiclassical or "first-order" Born-approximation-type calculations, was by Mu-Tao and McKoy [48] for the DCSs and ICSs of the $b'\ ^1\Sigma_u^+$ and $c_4'\ ^1\Sigma_u^+$ states using a distorted-wave approach. Notably good agreement was observed between the theoretical DCS data of Mu-Tao and McKoy [48] and the experimental DCS data of Khakoo *et al.* [34].

The lack of ICS data for these high-lying states can be attributed to a number of factors. Many N_2 electronic states lie very close to each other in energy. As such, vibronic EEL features associated with these states are heavily overlapped in the measured EEL spectra and require high-resolution measurements to be reliably unfolded. This becomes more difficult experimentally as the energy converges toward the ionization continuum. Practical limitations on energy resolution versus sufficient signal rate through multiple-scattering angles further constrain measurement capabilities. Moreover, the strong Rydberg-valence coupling of N_2 singlet *ungerade* states results in a heavy mixing of wave functions with a large rotational dependence (see Liu *et al.* [7], Heays *et al.* [49], and references therein for detailed discussions). Therefore, one cannot rely on calculated FCFs—using numerical methods such as the diabatic Rydberg-Klein-Rees (RKR) work of Whang *et al.* [50]—to simplify the unfolding of EEL spectra as has been typically applied to the analysis of lower-lying states in N_2 [10,45,51] as well as other molecules such as H_2 [52].

The ICSs of Trajmar *et al.* [16] relied on excitation energies and "effective" FCFs determined by combining the unity sum rule for FCFs with the relative EEL intensities measured by Geiger and Schröder [53] (at $E_0 = 25$ keV) and Joyez *et al.* [54] (at $E_0 = 14.3$ eV) (and references therein) for the

singlet and triplet states, respectively. Ratliff *et al.* [46] also employed FCFs in determining their $b\,^1\Pi_u$ state ICSs at 60 and 100 eV while only explicitly fitting the $v' = 1$–3 levels in their EEL data. Due to the presence of strong Rydberg-valence interactions mentioned above [7,49], this application of the relative intensities is not accurate. The present ICS work, based on the DCSs of Khakoo *et al.* [34], thus should be regarded as more reliable than previous measurements.

Recently, Kato *et al.* [20] measured N_2 EEL spectra at scattering angles of 10° and 20° at E_0 values of 20, 30, and 40 eV. This was an important effort "to try and shed light on the worrying discrepancies that exist in the literature for the $a\,^1\Pi_g$, $C\,^3\Pi_u$, $E\,^3\Sigma_g^+$, and $a''\,^1\Sigma_g^+$ cross sections." Their measurements demonstrated reasonable consistency with our recent work [10,11,34] for the $a\,^1\Pi_g$, $C\,^3\Pi_u$, $E\,^3\Sigma_g^+$, $a''\,^1\Sigma_g^+$, $b\,^1\Pi_u$, $c_3\,^1\Pi_u$, and $G\,^3\Pi_u$ states (and presumably the $A\,^3\Sigma_u^+$, $B\,^3\Pi_g$, $W\,^3\Delta_u$, $B'\,^3\Sigma_u^-$, $a'\,^1\Sigma_u^-$, and $w\,^1\Delta_u$ states), but Kato *et al.* [20] concluded that agreements for the $o_3\,^1\Pi_u$, $b'\,^1\Sigma_u^+$, $c_4'\,^1\Sigma_u^+$, and $F\,^3\Pi_u$ states were not as satisfactory. Reasons for differences in the data of Kato *et al.* [20] compared to the data of Khakoo *et al.* [34] may include the usage of the movable gas source by Khakoo *et al.* [34] that provides a superior background scattering signal removal. The sparse sampling of the DCSs in Ref. [20], even though it made use of a similarly narrow angular acceptance to that used for the present work, caused difficulty in extrapolating differences (specifically on steep DCS regions, i.e., $\theta \sim 10°$ for the $o_3\,^1\Pi_u$, $b'\,^1\Sigma_u^+$, and $c_4'\,^1\Sigma_u^+$ states) to the entire angular range of the DCSs and the corresponding contribution to the ICSs. While the end result of the unfolding procedure employed in Ref. [20] is explained to be similar to that applied in Ref. [34], the EEL unfolding methods remain complicated and likely contribute to differences in the measured results (certainly for the $b'\,^1\Sigma_u^+$ state), particularly given the distinctly different EEL ranges unfolded (i.e., different vibronic inclusion): up to ∼13.8 eV in Ref. [34] and ∼15.2 eV in Ref. [20]. Again, we note that EEL unfolding becomes even more challenging as the upper limit of the EEL coverage approaches the ionization potential.

In the EEL measurements of Heays *et al.* [49], the target N_2 beam was formed by effusing the gas through a thin aperture source (see Khakoo *et al.* [55]) instead of the previous capillary array of Khakoo *et al.* [34]. While providing a simpler conceptualization of the scattering volume as a function of angle, the measured inelastic-to-elastic scattering intensity ratios employed in both analyses effectively nullify any scattering volume variations between the two gas beam methods. Heays *et al.* [49] included EEL measurements at E_0 values of 30, 50, and 100 eV, for θ values of 1°–90°, at higher resolution (≈30 meV) and a lower electron current of about 5 nA compared to Ref. [34] (≈40–50 meV at ∼7–10 nA).

There was an additional important distinction in the EEL measurements of Heays *et al.* [49] compared to Khakoo *et al.* [34]: The detection analyzer system was nontrivially modified. Instead of using physical apertures at the front nose cone of the device, a virtual aperture system was used. Specifically, the cylindrical nose cone of Ref. [34], with a pair of 1-mm-diam apertures, was replaced by a "conical funnel" nose piece composed of a narrow front opening (3.5 mm in diameter) widening to a back aperture of the same throughput diameter, effectively forming a "skimmer" of rogue electrons. In addition, two solid angle defining apertures (pupil-window combination), each 0.7 mm in diameter, were placed 20 mm apart within the field-free body of a downstream lens (i.e., forming a virtual aperture system), providing an angular resolution of ∼2° full width at half maximum (FWHM). The virtual aperture configuration enabled electrons with scattered kinetic energies less than 5 eV to be transmitted significantly more efficiently through the detector than the previous arrangement. In particular, this improved setup enabled our system to perform better at lower E_0 where the scattered electrons predominantly had kinetic energies <5 eV. The skimmer apertures served to limit the depth of field of the spectrometer to a region of roughly ± 4 mm about the center of the collision region. For higher-energy work (i.e., Refs. [34,49]), this is not as relevant, but it still means that the apparatus was significantly changed from its earlier configuration. Regardless of these significant equipment differences, the EEL spectra measured by Khakoo *et al.* [34] and Heays *et al.* [49] were in good agreement within uncertainties, and with a better consistency than shown between Kato *et al.* [20] and Khakoo *et al.* [34]. This may largely reflect the subtle differences in the EEL unfolding methods of our work and that of Kato *et al.* [20], rather than an inherent difference in the measured EEL data. We note that the sum of DCSs of Khakoo *et al.* [34] divided by the sum of DCSs of Heays *et al.* [49], for the $b\,^1\Pi_u$, $c_3\,^1\Pi_u$, $o_3\,^1\Pi_u$, $b'\,^1\Sigma_u^+$, $c_4'\,^1\Sigma_u^+$, $G\,^3\Pi_u$, and $F\,^3\Pi_u$ states, were 1.098, 1.077, and 1.060, respectively, for E_0 values of 30, 50, and 100 eV. These represent minor differences, easily within assigned uncertainties, between the EEL results of Khakoo *et al.* [34] and Heays *et al.* [49]. The ratios for individual electronic states are also within the assigned DCS uncertainties of Khakoo *et al.* [34]. Consequently, we expect that the presently reported ICSs should be a considerable improvement over past ICSs.

III. INTEGRAL CROSS SECTIONS

The present ICSs were derived from the DCSs of Khakoo *et al.* [34] in a manner similar to that described by Johnson *et al.* [9] and Malone *et al.* [12]. Full experimental details and an extensive discussion of the EEL and DCS analysis can be found in Khakoo *et al.* [34]. We note here that we later determined that the 17.5-eV $a''\,^1\Sigma_g^+$ state DCSs of Ref. [34] required correction (an upward scaling by 1.295) due to a transmission issue [11]. This correction was also applied to the $b\,^1\Pi_u$, $c_3\,^1\Pi_u$, $o_3\,^1\Pi_u$, $b'\,^1\Sigma_u^+$, $c_4'\,^1\Sigma_u^+$, $G\,^3\Pi_u$, and $F\,^3\Pi_u$ state DCSs of Ref. [34] at 17.5 eV prior to determining the present 17.5-eV ICSs. Furthermore, interpolations between available DCSs and extrapolation to 0° scattering, where the forwardmost scattering DCS was not directly measured due to experimental constraints, were performed using a B-spline algorithm. Unfortunately, there is a paucity of reliable theoretical predictions of the relevant angular distributions for all the excitations covered in this work. Therefore, extrapolations to experimentally inaccessible backward scattering angles were determined by (essentially) visually assessing the trends suggested in the measured DCS data. Given the large angular coverage of the DCSs employed (up to 130°), the forward peaked nature of many of the presently investigated cross sections, and the $\sin(\theta)$ factor that is introduced into the

TABLE I. Normalized relative excitation probabilities (REPs) taken from the experimental work of Khakoo *et al.* [34] (as based on the coupled (nonadiabatic) results of Stahel *et al.* [72]; see Table I(b), "P(renorm)" values, and Table IV, "scaling factor" values, in Ref. [34]) for electron-impact excitation of the $b\ ^1\Pi_u$, $c_3\ ^1\Pi_u$, $o_3\ ^1\Pi_u$, $b'\ ^1\Sigma_u^+$, and $c_4'\ ^1\Sigma_u^+$ states from the $X\ ^1\Sigma_g^+$ ($v' = 0$) ground-state level in N_2. These REPs are used to account for unmeasured vibrational levels and enable conversion of the present *partial* ICSs (measured portion given by the "Sum" values) into *full* ICSs over all vibrational levels. See text for further discussion.

	$b\ ^1\Pi_u$		$c_3\ ^1\Pi_u$		$o_3\ ^1\Pi_u$		$b'\ ^1\Sigma_u^+$		$c_4'\ ^1\Sigma_u^+$	
v' level	REP	Error	REP	Error	REP	Error	REP	Error	REP	Error
Sum	0.973	0.036	1.000	0.136	0.912	0.314	0.081	0.019	0.825	0.025
0	0.014	0.001	0.494	0.063	0.024	0.023	0.009	0.002	0.785	0.025
1	0.051	0.003	0.391	0.119	0.343	0.148	0.011	0.014	0.034	0.002
2	0.123	0.007	0.110	0.017	0.224	0.173	0.001	0.001	0.002	0.003
3	0.215	0.010	0.004	0.001	0.321	0.216	0.004	0.001	0.004	0.002
4	0.281	0.022					0.003	0.003		
5	0.012	0.008					0.003	0.001		
6	0.032	0.010					0.005	0.002		
7	0.090	0.012					0.003	0.001		
8	0.005	0.001					0.020	0.011		
9	0.026	0.015					0.014	0.003		
10	0.053	0.007					0.008	0.002		
11	0.020	0.001								
12	0.014	0.004								
13	0.033	0.008								
14	0.004	0.004								

integration by the spherical volume element, the contribution of the extrapolated region (up to 180°) of the DCS curve to the resulting ICS is minimized. We note that the shapes of the $b'\ ^1\Sigma_u^+$ and $c_4'\ ^1\Sigma_u^+$ state DCSs of Mu-Tao and McKoy [48] agreed excellently with those of Khakoo *et al.* [34], substantiating our extrapolations to 180°.

In order to assess the total uncertainties in the derived ICSs, the uncertainty in the interpolation and extrapolation procedures was estimated as follows. No uncertainty in the resulting ICSs was attributed to the interpolation between measured points due to the dense angular coverage of the DCSs (see Khakoo *et al.* [34]). Further, uncertainties related to extrapolations of the DCSs to 0° scattering were also considered negligible due to the minimal angular extent of the extrapolations (<3°) and the rapid convergence of the $\sin(\theta)$ factor toward zero as $\theta \rightarrow 0°$. Extrapolations over the backward scattering angles did provide a potentially significant contribution to the overall uncertainties of the derived ICSs. This occurred particularly at smaller electron-impact energies for the dipole-allowed transitions, which were not intensely forward peaked in this work. In all cases, multiple independent integrations (at least two per state) were performed to guide the error estimates. Along with the "properly" extrapolated DCSs used to generate the final ICS values, ICSs were determined by integrating DCSs with "worst-case" extrapolations applied (i.e., DCS held constant from the last measured angle out to 180°). The difference between the ICSs determined using the two extrapolations was taken as the uncertainty contributed from the extrapolation procedure. These extrapolation errors were then combined in quadrature with the average uncertainty of the DCSs being integrated to give the total uncertainty quoted for the resulting ICSs. ICSs for particular vibronic transitions, such as the $X\ ^1\Sigma_g^+$ ($v' = 0$) – $c_4'\ ^1\Sigma_u^+$ ($v' = 0$) excitation (see Sec. IV E), also included the uncertainty of the relative excitation probabilities (REPs, which are effectively pseudo-FCFs) stated in Table I(a) of Ref. [34] and summarized in Table I of the present work. Note that CSE-determined REPs will be more accurate than the REPs in Table I when additional photoabsorption and CSE data become available for more v' levels of Rydberg-valence states. We also note that the majority of the total uncertainty was typically due to the measured DCS contributions, not the angular extrapolations, for the presently covered Rydberg-valence states.

It should also be pointed out that the "transmission correction" of N_2 for the instrumental response function of the detector that was applied in Ref. [34] may be in question for the 17.5- and 20-eV results. (At larger E_0, the He transmission function was used and should not be in question [34,49].) This transmission correction was based on the EEL time-of-flight (TOF) measurements of LeClair and Trajmar [56], who determined absolute inelastic differential electron scattering cross sections at near-threshold impact energies for a 90° scattering angle partitioned over three EEL regions. Region III (12.4–13.5 eV) included the $b\ ^1\Pi_u$, $G\ ^3\Pi_u$, $D\ ^3\Sigma_u^+$, $c_3\ ^1\Pi_u$, $c_4'\ ^1\Sigma_u^+$, $F\ ^3\Pi_u$, $o_3\ ^1\Pi_u$, and $b'\ ^1\Sigma_u^+$ states for E_0 values between 14 and 20 eV. An additional EEL structure was observed, but not analyzed, between region III and the ionization threshold for larger electron-impact energies. Figure 5 of LeClair and Trajmar [56] illustrates substantially increased noise from signal compression for region III due to the t^3 factor in converting the scattering intensity from the TOF domain (as measured) to the EEL domain (convenient for unfolding analysis and comparison to typical EEL measurements). The ±50% relative uncertainty, assigned to the elastic-to-inelastic scattering intensity ratios of region III, is much larger than the ±5% and ±15% for regions I and II, respectively, and was taken into account within the DCS uncertainty estimations [34]. Unfortunately, there is no way at present to firmly

gauge the systematic uncertainty in Ref. [56] unless new TOF data becomes available. Consistency checks using repeated EEL experiments to minimize the statistical uncertainty and uncover and/or reduce other systematic errors, as well as utilizing more accurate normalizing elastic cross sections, can provide improvement to the uncertainty in these Rydberg-valence ICSs. Consequently, the present ICS uncertainties at 17.5 and 20 eV, as well as the corresponding DCSs of Khakoo *et al.* [34], may be underestimated. Newer "uniform transmission" EEL results for N_2, as discussed preliminarily in Ref. [57], which would improve the transmission correction of these low-energy cross sections (or at least confirm Ref. [56]), are needed.

IV. RESULTS AND DISCUSSION

Since the review of Trajmar *et al.* [16], various articles have been published providing reviews and recommendations for N_2 cross sections, e.g., Itikawa *et al.* [41], Majeed and Strickland [42], Itikawa [40], and Tabata *et al.* [43]. In terms of low E_0 measurements using the EEL method within the "few eV below ionization threshold" range (∼12.5–15.58 eV), very few EEL publications are available (e.g., Refs. [54,58–60]), with even fewer EEL-based DCSs and ICSs published. An early Born-approximation calculation by Chung and Lin [61] included excitation of the $b\,^1\Pi_u$, $b'\,^1\Sigma_u^+$, $c_4'\,^1\Sigma_u^+$, and $D\,^3\Sigma_u^+$ states. Hazi [62] calculated excitation of the $b'\,^1\Sigma_u^+$ and $c_4'\,^1\Sigma_u^+$ states using both a Born-approximation and semiclassical impact parameter method, while Mu-Tao and McKoy [48] calculated the DCSs and ICSs of the $b'\,^1\Sigma_u^+$ and $c_4'\,^1\Sigma_u^+$ states using a distorted-wave approach. As stated earlier, a previous "complete" set of excitation cross sections in this EEL range were those of Chutjian *et al.* [44] (DCSs and ICSs for the $b\,^1\Pi_u$, $c_3\,^1\Pi_u$, $o_3\,^1\Pi_u$, $b'\,^1\Sigma_u^+$, $c_4'\,^1\Sigma_u^+$, $G\,^3\Pi_u$, and $F\,^3\Pi_u$ states at E_0 values of 40 and 60 eV). Again, we emphasize that the Chutjian *et al.* [44] data was later renormalized by Trajmar *et al.* [16] aforementioned as a result of improved elastic cross sections that were used in their normalization process. Consequently, we refer to the DCS and ICS data of Trajmar *et al.* [16], rather than the original Chutjian *et al.* [44] data. Also, we have not applied the v'-level REP adjustment to EEL data, other than our own, whereby EEL measurements and theoretical calculations by other groups are provided as published.

Electron swarm results, as discussed in Brunger and Buckman [63], "have an important role to play in the checking for self-consistency of a given cross-section set. In this case, the "known" cross-section set can be used in conjunction with the Boltzmann equation to derive transport parameters, which are then compared against those measured in the swarm experiments. In this way the self-consistency of this cross-section set can be assessed." The swarm technique has been used (e.g., Refs. [14,64–66]) to generate scaling factors for excitation cross sections (of Trajmar *et al.* [16], for instance), as well as swarm transport parameters, of the inelastic states of N_2. However, we do not include $e^- + N_2$ swarm results in this Rydberg-valence state discussion since they are essentially scaled versions of data already discussed.

In the following discussion, renormalization of excitation cross sections has been performed (where stated) due to revisions of the applicable emission cross-section standards. The emission cross section σ_{em} is related to the (direct) excitation cross section (i.e., ICS) σ_{ex}, the cascade cross section σ_{casc}, and the predissociation cross section σ_{pre} as follows:

$$\sigma_{em} = \sigma_{ex} + \sigma_{casc} - \sigma_{pre}. \quad (1)$$

Alternatively, if the predissociation yield η is known, where $\sigma_{pre} = \eta\sigma_{ex}$, then Eq. (1) may be expressed (assuming negligible cascade contributing) as follows:

$$\sigma_{ex} = \sigma_{em}/(1-\eta). \quad (2)$$

In the cases discussed here, i.e., excitation to singlet *ungerade* states, any cascade must come (directly) from higher-lying (in energy) singlet *gerade* states. However, the excitation cross sections for these higher singlet *gerade* states, while poorly known, should be small given the *gerade* nature of the N_2 ground state. Therefore, the assumption inherent in Eq. (2) is well justified. Thus, Eq. (2) indicates that the excitation cross section may be directly renormalized using revised emission standards. These renormalizations implicitly assume that the spectral intensity calibration across expansive wavelength ranges is accurate in the original publications. The H Lyman-α emission standard at 121.6 nm arising from electron impact of H_2 was taken from the recommended values given in McConkey *et al.* [67] (see their Table 4.1.6.2a). We note that the Lyman-α recommendation of Ref. [67] used an unweighted average of accurate values from four independent measurements, similar to the methodology of van der Burgt *et al.* [68]. It is our opinion that this is a more reliable method than "arbitrarily" selecting one cross-section data set as "best" (e.g., as in Ref. [69]). The N I ($2p^3\,^4S^o$–$3s\,^4P$) electron-impact-induced emission standard at 120.0 nm from N_2 was taken from the recommendation of Malone *et al.* [70] (see their Table 1), which is self-consistent with the Lyman-α emission standard of McConkey *et al.* [67] within uncertainties.

Vibrationally resolved emission-based measurements depend on the relative intensities of vibrational contributions (e.g., see Table 1 in Zipf and McLaughlin [71]) determined from other data sources, such as by Geiger and Schröder [53], to account for the significant predissociation and effectively provide a more complete way to extrapolate to an excitation cross section. However, the Geiger and Schröder [53] experimental data show discrepancies when compared to the semiempirical coupled results of Stahel *et al.* [72] (as well as the photoabsorption measurements of Stark *et al.* [5] and the CSE calculations of Heays *et al.* [73]) that are expected to be more accurate. These discrepancies were likely due to the misassignment of vibrational levels (energies) that is largely a consequence of the resolution-limited EEL results (∼10 meV FWHM). Consequently, it is probable that inaccuracies in the unfolded intensities (i.e., effective FCFs) of Ref. [53] resulted, compared to the coupled work of Stahel *et al.* [72] (see their Tables II and IV and Fig. 4, as well as Table I in Khakoo *et al.* [34]). A thorough vibronic reevaluation of previously published emission results is difficult and beyond the scope of this work. As a consequence, the spectral overlap of blended emission features in past works is not reevaluated here. Also, reassessment of predissociation per (v,J) level is

not attempted as a means of providing a more accurate cross section. New rotationally resolved measurements and analysis are a better approach to providing accurate emission-based excitation cross sections.

In general, the electron-impact emission technique is superior to EEL measurements from a wavelength (energy-loss) *resolution* point of view; however, the significantly greater number of contributing features in emission measurements can be a serious impairment, particularly when significant cascading and predissociation (as well as autoionization) are involved. Thus, based on these factors, the present EEL measurement approach can be considered to be better over standard emission-based measurements (e.g., Ajello *et al.* [74] and James *et al.* [36]), critically so for the $c_3\,{}^1\Pi_u$ and $o_3\,{}^1\Pi_u$ states, where optical emission is too weak. Another improvement is the modified-Born method, which utilizes the measured excitation function (i.e., relative emission intensity as a function of E_0) and the optical oscillator strengths (OOSs), using complimentary techniques such as the present emission-based excitation cross-section determinations discussed below. The present excitation cross-section estimation method utilized the measured emission-based excitation shape function of the $b\,{}^1\Pi_u$ state (see James *et al.* [36]) or of the $c_4'\,{}^1\Sigma_u^+$ state (see Ajello *et al.* [74]). Also, the CSE-optimized OOSs of Heays *et al.* [73] and Stark *et al.* [5,8] were used for absolute cross-section normalization in the high-energy region (of the Born limit). Here, a modified Born-approximation model (see Refs. [36,74] and references therein) was used with experimentally determined energy levels (e.g., Refs. [37–39,75–78]) to calculate individual threshold energies of each $(0,J'') \rightarrow (v',J')$ transition (accurate to a fraction of cm^{-1}) and weighted according to the relative $X\,{}^1\Sigma_g^+(0,J'')$ population at 300 K. Since the OOSs of high v' levels are not reliably known, care should be taken to ensure that the particular v-level ranges used are stated to enable meaningful comparison between (partial) excitation cross sections determined using different techniques.

A. The $b\,{}^1\Pi_u$ state

The $b\,{}^1\Pi_u$ state has a relatively large cross section as shown in Fig. 1, with the present values provided in Tables II and III. The present ICSs are shown for both the measured partial ($v' = 0$–14) and REP-based "full" ($v' = 0$–19) contributions, where the partial (measured) contribution represents 97.3% of the cross section (see Table I). Also shown in Fig. 1 are the excitation cross sections of Ajello *et al.* [2], Ratliff *et al.* [46], James *et al.* [36], Trajmar *et al.* [16], and Zipf and Gorman [79] from near threshold to >100 eV. Renormalization of the cross sections of James *et al.* [36] and Zipf and Gorman [79] were performed: James *et al.* [36] was adjusted by the factor 7.03/7.3 (Lyman-α from H_2 [67,69]) and Zipf and Gorman [79] was adjusted by 3.7/6.7 (N I 120.0 nm from N_2 [70,80]). The recent cross section of Ajello *et al.* [2] for the $b\,{}^1\Pi_u$ state, which is an unchanged reevaluation of previous emission and predissociation data by Ajello and co-workers (see James *et al.* [36], Table 6), was not renormalized in the present work. This indicates the relatively small change to the James *et al.* [36] data resulting from the revised Lyman-α cross section.

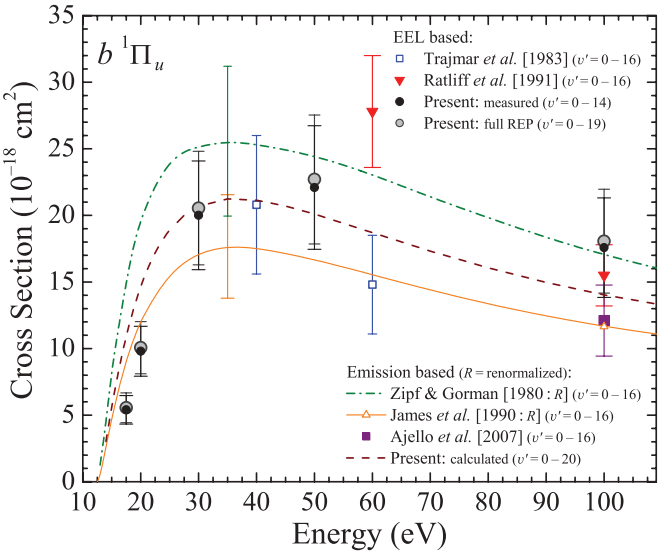

FIG. 1. (Color online) Cross sections for electron-impact excitation of the $b\,{}^1\Pi_u$ state in N_2. The legend is displayed in the figure.

The present emission-based estimation to the $b\,{}^1\Pi_u$ state excitation cross section, covering $v' = 0$–20 (equivalent to the present "full" ICS), was determined as discussed immediately above Sec. IV A and is shown in Fig. 1. From this we see good agreement between the present results, particularly near the peak of the excitation cross section. The present calculated excitation cross section roughly splits the difference between the emission-based excitation cross sections of Zipf and Gorman [79] and James *et al.* [36].

Figure 1 shows the ICSs of Trajmar *et al.* [16] (presumably covering $v' = 0$–16, based on Fig. 1–3 of Chutjian *et al.* [44]), noting that we adjusted (upward) a presumed typographical error (i.e., 4.8, also shown adjusted in Fig. 2 of Ref. [46]) to be 14.8×10^{-18} cm^2 at 60 eV. The 40-eV ICS of Trajmar *et al.* [16] agrees well with the present data, but their 60-eV ICS value is somewhat lower, suggesting a sharper falloff than the present data indicate.

The ICSs of Ratliff *et al.* [46] (presumably covering $v' = 0$–16) were obtained at 60 and 100 eV via DCSs derived from EEL measurements with a resolution of roughly 50-meV FWHM. Comparing data sets in Fig. 1 suggests that their 60-eV ICS may be too large while the present 100-eV ICS also may be too large. Ratliff *et al.* [46] used only their measured $v' = 1$–3 levels of the $b\,{}^1\Pi_u$ state (they listed up to $v' = 14$) along with the vibrational level energies and relative intensities of Geiger and Schröder [53] (tabulated up to $v' = 16$) to obtain a "total" $b\,{}^1\Pi_u$ state contribution. However, their DCSs are not provided in Ref. [46], making assessment of the DCS extrapolation to large θ impossible, which seriously diminishes their ICS reassessment. Furthermore, the results of Heays *et al.* [49] suggest that extrapolating the relatively few v levels measured ($v' = 1$–3) to all v levels would be problematic (potentially nonuniform with respect to E_0) depending on the particular scattering momenta. Ratliff *et al.* [46] also mentioned a potential discrepancy within the Zipf and Gorman [79] data (see the James *et al.* [36] discussion below); however, the general lack of details in their paper [46]

TABLE II. ICSs for electron-impact excitation of the $b\,^1\Pi_u$ ($v' = 0$–14), $c_3\,^1\Pi_u$ ($v' = 0$–3), $o_3\,^1\Pi_u$ ($v' = 0$–3), $b'\,^1\Sigma_u^+$ ($v' = 0$–10), $c_4'\,^1\Sigma_u^+$ ($v' = 0$–3), $G\,^3\Pi_u$ ($v' = 0$–3), and $F\,^3\Pi_u$ ($v' = 0$–3) states from the $X\,^1\Sigma_g^+$ ($v' = 0$) ground-state level in N_2 (unit: 10^{-18} cm^2). These ICSs were derived from the DCS measurements of Khakoo *et al.* [34]. Note that these states are *partial* ICSs in terms of the vibrational (v') contributions. The $b'\,^1\Sigma_u^+$ state was included for completeness even though only a minor vibronic contribution (see Table I) of its intensity was measured. The $c_3\,^1\Pi_u$, $G\,^3\Pi_u$, and $F\,^3\Pi_u$ states are essentially full ICSs in terms of the contributing v' levels. Also, a correction to the $a''\,^1\Sigma_g^+$ state DCSs of Ref. [34] at 17.5 eV (scaled upward by 1.295 as discussed in Malone *et al.* [11]) due to a transmission issue (see Sec. III) was also applied to the present ICSs at 17.5 eV. See text for further discussion.

Energy	$b\,^1\Pi_u$		$c_3\,^1\Pi_u$		$o_3\,^1\Pi_u$		$b'\,^1\Sigma_u^+$		$c_4'\,^1\Sigma_u^+$		$G\,^3\Pi_u$		$F\,^3\Pi_u$	
(eV)	ICS	Error	ICS	Error	ICS	Error	ICS	Error	ICS	Error	ICS	Error	ICS	Error
17.5	5.40	1.07	2.06	0.43	1.50	0.34	1.97	0.46	1.05	0.25	1.65	0.44	0.753	0.213
20	9.80	1.87	3.52	0.69	2.29	0.48	2.48	0.54	1.79	0.41	1.68	0.46	0.900	0.250
30	20.0	4.1	7.53	1.57	3.36	0.71	3.33	0.73	5.07	1.17	1.92	0.50	1.32	0.36
50	22.1	4.6	10.1	2.2	4.97	1.07	4.63	1.07	7.01	1.70	1.58	0.44	0.835	0.249
100	17.6	3.7	8.53	1.85	4.92	1.05	3.26	0.78	7.90	1.98	0.587	0.192	0.336	0.119

makes for a difficult assessment and it should be pointed out that their comparative cross-section plot apparently does not show renormalized data for other measurements (e.g., Zipf and Gorman [79]). A predissociation branching ratio of approximately 0.962 was stated by Ratliff *et al.* [46] via a comparison with the 100-eV emission data of James *et al.* [36]; a similar procedure generates a value of approximately 0.967 for the present ICS data.

Ajello *et al.* [2] reevaluated their previous emission and predissociation data by Ajello and co-workers with no change made to the original $b\,^1\Pi_u$ ($v' = 0$–16) state cross section, which was tabulated by them in Ref. [36] (see their Table 6). As discussed above, renormalization of the Ajello *et al.* [2] data would agree with the 100-eV cross section of the renormalized James *et al.* [36] data shown in Fig. 1 since the reevaluation resulted in no change. Though the Lyman-α revised recommendation induces a small adjustment to the Ajello *et al.* [2] and James *et al.* [36] cross-section values, it needs to be utilized. The 100-eV cross section of Ajello *et al.* [2] is slightly smaller than the present, but agrees within experimental uncertainties. Likewise, the renormalized 100-eV cross section of James *et al.* [36] agrees with the present ICS within uncertainties.

The $b\,^1\Pi_u$ ($v' = 0$–16) excitation shape function of James *et al.* [36], from threshold to >100 eV, was constructed using their published parameters (see their Table 4) for the modified Born approximation [81,82]. This was scaled using their renormalized 100-eV cross-section data point. They also stated a predissociation fraction of ~0.949 for $b\,^1\Pi_u$ ($v' = 0$–16) and ~0.105 for $b\,^1\Pi_u$ ($v' = 1$). While the excitation function shape was based on the $b\,^1\Pi_u$ ($v' = 1$) $\rightarrow X\,^1\Sigma_g^+$ ($v'' = 2$) emission intensity (at 103.28 nm) as a function of E_0, their ability to properly account for predissociation of high J levels of $b\,^1\Pi_u$ ($v' = 1$) leads to questions of their cross-section accuracy. Additionally, issues with determining the relative sensitivity of the optical detection system (discussed further in Sec. IV E) and overlapping among emission features are potentially problematic. The spectral resolution used in James *et al.* [36] (and Ajello *et al.* [74]) was insufficient to resolve emission features in numerous instances, thus causing difficulty in partitioning particular emission intensities into different spectral components. A detailed comparison of the tabulated data in both James *et al.* [36] and Ajello *et al.* [74] leads to inconsistencies in their partitioning of blended emission features, but also probable inconsistencies in the summation of individual vibronic intensities with some possible double counting. For instance, this is realized by summing their measured emissions for various $v' \rightarrow v''$ from their first table in each paper and comparing with values in subsequent tables.

James *et al.* [36] partially obtained their absolute excitation cross section at 100 eV by rescaling and reanalyzing portions of the 200-eV results of Zipf and Gorman [79], which depended on the measured relative intensities (at $E_0 =$ 25 keV) of Geiger and Schröder [53]. The modified Born-approximation procedure used in James *et al.* [36], which

TABLE III. ICSs for electron-impact excitation of the $b\,^1\Pi_u$, $c_3\,^1\Pi_u$, $o_3\,^1\Pi_u$, $b'\,^1\Sigma_u^+$, and $c_4'\,^1\Sigma_u^+$ singlet *ungerade* states from the $X\,^1\Sigma_g^+$ ($v' =$ 0) ground-state level in N_2 (unit: 10^{-18} cm^2). These *full* ICSs, which include "all" vibrational (v') levels, were determined by applying the REP scaling factors (see Table I) to the *partial* ICSs of Table II. The $b'\,^1\Sigma_u^+$ state "full" ICSs were estimated as explained in Sec. IV D. The $b'\,^1\Sigma_u^+$ state error values do not include any uncertainty estimation for the scaling method applied in this instance. See text for further discussion.

Energy	$b\,^1\Pi_u$		$c_3\,^1\Pi_u$		$o_3\,^1\Pi_u$		$b'\,^1\Sigma_u^+$		$c_4'\,^1\Sigma_u^+$	
(eV)	ICS	Error	ICS	Error	ICS	Error	ICS	Error	ICS	Error
17.5	5.55	1.12	2.06	0.43	1.64	0.68			1.28	0.31
20	10.1	2.0	3.52	0.69	2.52	1.02			2.17	0.50
30	20.6	4.3	7.53	1.57	3.68	1.49	*9.16*	*2.02*	6.15	1.43
50	22.7	4.8	10.1	2.2	5.45	2.22	*12.7*	*2.9*	8.50	2.08
100	18.1	3.9	8.53	1.85	5.39	2.19	*8.96*	*2.14*	9.58	2.42

enabled calculation of excitation cross sections for particular vibrational progressions, utilized vibronic energies from Stahel *et al*. [72], which should be an improvement over the earlier usage of data from Geiger and Schröder [53]. Also, the cross sections of James *et al*. [36] appear to be systematically lower from the near-peak region to larger E_0, as shown in Fig. 1, but agrees with the present data within uncertainties at all common energies except near 17.5 eV. As mentioned above within the Ratliff *et al*. [46] discussion, it was suggested that the reassessed Zipf and Gorman [79] emission cross section for the $b\,^1\Pi_u\,(v'=1)$ progression should be ∼46% larger than the data of James *et al*. [36], but as James *et al*. [36] conceded, there are too few details within Zipf and Gorman [79] to provide a fully adequate reassessment. Consequently, as discussed above, we renormalized the published values of Zipf and Gorman [79] based only on revised emission standards.

Good agreement between the present data and the cross section (apparently covering $v'=0$–16) of Zipf and Gorman [79] is evident for the shape and magnitude within uncertainties (assumed to be 22%), from approximately the peak region (>30 eV) to larger E_0, but they appear too large at smaller E_0 compared to all other data shown in Fig. 1. The scaled shape of Zipf and Gorman's cross section [79] agrees very well with James *et al*. [36] from near peak to >400 eV, but some disagreement from threshold to the peak region exists. We point out that an average of the emission-based excitation cross sections of Zipf and Gorman [79] and James *et al*. [36] agree excellently with the present results, which is born out via the presently calculated emission-based excitation cross section. These excitation cross sections involve very large predissociation branching ratios (e.g., >0.92 for the $b\,^1\Pi_u$ state as a whole [79]) with essentially all emission stemming from low J levels of the $b\,^1\Pi_u$ $(v'=1)$ state. [Note that CSE calculations and experiment indicate the high J levels of $b(1)$ also have a significant predissociation yield [33].] The large predissociation fraction suggests that the emission-based measurements performed at vibrational resolutions seriously underestimate the uncertainties in the derived excitation cross sections. This is partly due to compounding uncertainties in the conversion to excitation cross sections; see the Geiger and Schröder [53] discussion above. The considerable perturbations present within these states at the rotational level (see Stahel *et al*. [72], Liu *et al*. [7], and Heays *et al*. [49] for further discussion), where the particular populations are temperature dependent, is the basis for the significant values of these predissociation factors.

Also of note is the emission-based cross-section data of Zipf and McLaughlin [71], which utilized the relative intensities of the EEL data of Geiger and Schröder [53] to extrapolate to the "full" range of vibrational contributions, with a stated total $(v'=0$–$13)$ excitation cross section of 20.7×10^{-18} cm^2 at 200 eV. If we reasonably assume the same spectral calibration as in Zipf *et al*. [83] and Zipf and Gorman [79], then the factor 3.7/6.7 (N I 120.0 nm from N_2, see above) provides a renormalized cross section of 11.4×10^{-18} cm^2 at 200 eV, which is consistent with the renormalized data of Zipf and Gorman [79]. Similar to Ref. [79], Zipf and McLaughlin [71] also stated a predissociation branching ratio of 0.969. Additionally, Morgan and Mentall [84] measured the $b\,^1\Pi_u\,(v'=1)\rightarrow X\,^1\Sigma_g^+\,(v''=2)$ emission intensity (at 103.3 nm) at an E_0 value of 200 eV, as well as the $b(5,0)$ emission. Their companion O_2 work in Ref. [84] contained a serious (shape) error for the O II 83.4-nm emission cross section, as discussed by Malone *et al*. [85]. Consequently, caution is warranted for the Morgan and Mentall [84] data, though a renormalization (7.03/12.3 for Lyman-α from H_2 [67,86]) provides an adjusted *emission* cross section of 1.20×10^{-19} cm^2 at 200 eV for $b(1,2)$, which compares, for instance, to the corrected (N I 120.0 nm from N_2, see above) emission value 1.24×10^{-19} cm^2 at 200 eV of Zipf and Gorman [79].

In summary, although the scatter among excitation cross-section data sets is not yet acceptable, the situation is improved for the $b\,^1\Pi_u$ state compared to the early 1990s. Inclusion of high v' levels (i.e., $v'>16$) is not likely cause for disagreements between data sets. While the present ICS trend may be high at 100 eV, the consistency in the work of Heays *et al*. [49] suggests the present excitation cross section is accurate within overlapping uncertainty estimations.

B. The $c_3\,^1\Pi_u$ state

Essentially 100% of the $c_3\,^1\Pi_u$ state was observed (see Table I) within the unfolded EEL range of our experiment, where the measured partial $(v'=0$–$3)$ and REP-based full $(v'=0$–$4)$ contributions are shown in Fig. 2 from near threshold to 100 eV and listed in Tables II and III. Note that larger vibrational contributions, such as $v'=4$, are negligible (see Refs. [34,72]), where the sum of effective FCFs for $v'>3$ is less than ∼0.005%. Also shown in Fig. 2 are the data of Ajello *et al*. [2] and Trajmar *et al*. [16]. The data of Zipf and McLaughlin [71], which are partly based on the relative intensities of Geiger and Schröder [53] (see the discussion in Sec. IV A), are not displayed and have a renormalized (via N I 120.0 nm from N_2) total $(v'=0$–$7)$ excitation cross section

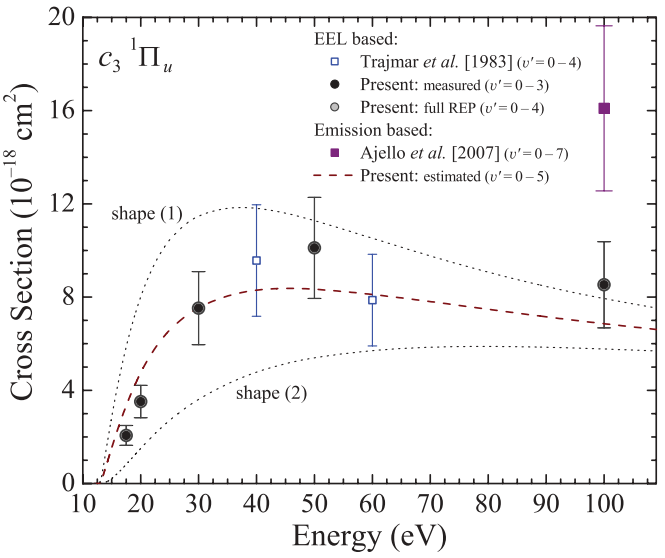

FIG. 2. (Color online) Cross sections for electron-impact excitation of the $c_3\,^1\Pi_u$ state in N_2. The black dotted curves represent the $b\,^1\Pi_u$ shape (1) and the $c_4'\,^1\Sigma_u^+$ shape (2), which are explained in the text. The legend otherwise indicates the plotted data.

of 6.63×10^{-18} cm^2 at 200 eV and a stated predissociation branching ratio of >0.99.

The ICSs of Trajmar *et al.* [16] demonstrate surprisingly good agreement with the present cross-section data, taking into consideration that they did not account for Rydberg-valence interactions in their spectra as aforementioned. The vibrational coverage of the ICSs of Trajmar *et al.* [16] are not explicitly stated, which appear to include $v' = 0$–4; however, their magnitude is consistent with the present data. Their excitation function shape, shown in Fig. 2, is reasonable within experimental uncertainties.

Figure 2 illustrates the disagreement (beyond uncertainties) in the cross section of Ajello *et al.* [2] with both the ICS data sets and the present emission-based estimation of the excitation cross section. Ajello *et al.* [2] reevaluated previous emission and predissociation data by Ajello and co-workers with no change to the original $c_3\,{}^1\Pi_u$ ($v' = 0$–7) state cross section tabulated by James *et al.* [36] (see their Table 6). The cross section of Ajello *et al.* [2] is larger than the present 100-eV data by a factor of ∼1.8 and a potential v'∼5–7 contribution is most likely insufficient to account for the difference. We note that Ajello *et al.* [2] (and James *et al.* [36]) stated a predissociation of 100% for the $c_3\,{}^1\Pi_u$ state, similar to Zipf and McLaughlin [71], which was mainly based on a comparison of their observed (optically thin) emissions with the EEL-derived relative intensity results of Geiger and Schröder [53] (see the above discussion). Also, in terms of possible cascade population feeding of the $c_3\,{}^1\Pi_u$ state, it was noted by Allen *et al.* [87] that the $y\,{}^1\Pi_g$ state is more likely to transition to the $w\,{}^1\Delta_u$ and $a'\,{}^1\Sigma_u^-$ states, or to the $o_3\,{}^1\Pi_u$ and $c_4'\,{}^1\Sigma_u^+$ states, rather than to the $c_3\,{}^1\Pi_u$ state. This is because the $y\,{}^1\Pi_g \rightarrow c_3\,{}^1\Pi_u$ transition would require a simultaneous change of two electron configurations [i.e., involving two active electrons, noting the configurations $(1\pi_u)^4(3\sigma_g)^1 3p\pi_u\, c_3\,{}^1\Pi_u$ and $(1\pi_u)^3(3\sigma_g)^2 4p\sigma_u\, y\,{}^1\Pi_g$ [35]], which is forbidden by the independent electron model. Additionally, possible branching of the $c_3\,{}^1\Pi_u$ state, for instance, via the $c_3(2) \rightarrow a(0)$ transition, which is blended with the $y(1) \rightarrow w(3)$ and $k\,{}^1\Pi_g(1) \rightarrow w(3)$ transitions, is likely to be very weak but definitely nonzero [87,88]. [Of note, Morgan and Mentall [84] claimed to have observed $c_3\,{}^1\Pi_u \rightarrow X\,{}^1\Sigma_g^+$ emissions, specifically $c_3(1,0)$, $c_3(1,1)$, and $c_3(1,3)$ at 200 eV, but their spectral resolution and previously discussed experimental issues are causes for concern whereby their observations need confirmation. However, Roncin *et al.* [37] observed $c_3(1,v'')$ and $c_3(2,v'')$ emissions in a discharge and Ajello [89] suggests various $c_3(v',v'')$ emissions were observed in recent work.] This indicates that the predissociation amount (100%) used by emission-based excitation cross-section estimations of the $c_3\,{}^1\Pi_u$ state (e.g., Ajello *et al.* [2]) may need adjustment, with a corresponding revision to the excitation values. Consequently, the disagreement between the cross-section data of Ajello *et al.* [2] compared to the present excitation cross sections and the ICSs by Trajmar *et al.* [16] is not clear at present.

Since the excitation function of the $c_3\,{}^1\Pi_u$ state cannot be measured with the typical emission-based method, the present attempt to estimate the $c_3\,{}^1\Pi_u$ state excitation cross section, covering $v' = 0$–5 (equivalent to the present "full" ICS), was determined in a similar way to that described previously (i.e., as discussed immediately above Sec. IV A), but using a hybrid-model approach for estimation purposes. Here, the excitation shape functions of the $b\,{}^1\Pi_u$ state [36] and the $c_4'\,{}^1\Sigma_u^+$ state [74] were independently used along with the CSE-optimized $c_3\,{}^1\Pi_u$ state OOSs [5,8,73]. The modified Born-approximation model shapes of the $b\,{}^1\Pi_u$ and $c_4'\,{}^1\Sigma_u^+$ states, both using the $c_3\,{}^1\Pi_u$ state OOS, were combined using an unweighted average, along with experimentally determined energy levels of the $c_3\,{}^1\Pi_u$ state. Figure 2 shows that the individual $b\,{}^1\Pi_u$ state [shape (1)] and $c_4'\,{}^1\Sigma_u^+$ state [shape (2)] excitation shapes are insufficient, while good agreement between the present results is observed for the hybrid (average) shape estimation, especially considering the significant approximations. Importantly, this analysis suggests a different energy for the maximum cross section of the Rydberg $3p\pi_u$ $c_3\,{}^1\Pi_u$ state compared to the valence $b\,{}^1\Pi_u$ state and Rydberg $c_4'\,{}^1\Sigma_u^+$ state.

C. The $o_3\,{}^1\Pi_u$ state

Available cross-section data on the $o_3\,{}^1\Pi_u$ state is very limited at this time. The present results and that of Ajello *et al.* [2] and Trajmar *et al.* [16] are shown in Fig. 3 from near threshold to 100 eV. The data of Zipf and McLaughlin [71], which are partly based on the relative intensities of Geiger and Schröder [53] (see the discussion in Sec. IV A), are not displayed and have a renormalized (via N I 120.0 nm from N_2) total ($v' = 0$–4) excitation cross section of 2.66×10^{-18} cm^2 at 200 eV with a stated predissociation branching ratio of >0.99. The present ICSs are shown for both the measured partial ($v' = 0$–3) and REP-based full ($v' = 0$–4) contributions, which are listed in Tables II and III, respectively. The partial (measured) contribution represents 91.2% of the cross section (see Table I). The larger error bars for the full versus partial cases of the present data is due to the relatively large (∼34%) estimated uncertainty attributed to the scaling factor used for correcting for the unmeasured signal (see Table I and

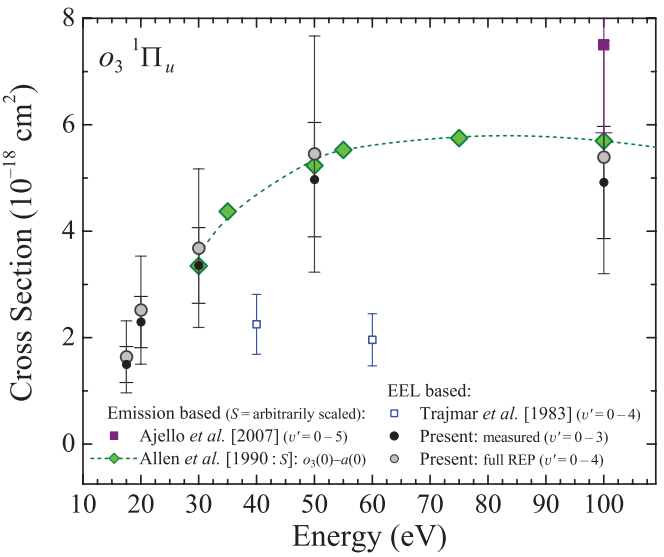

FIG. 3. (Color online) Cross sections for electron-impact excitation of the $o_3\,{}^1\Pi_u$ state in N_2. The arbitrarily scaled cross-section shape of Allen *et al.* [87] is from their measured optical emission cross section for the $o_3\,{}^1\Pi_u$ ($v' = 0$) → $a\,{}^1\Pi_g$ ($v' = 0$) transition.

Khakoo *et al.* [34], Table IV). This stems from the $o_3\ ^1\Pi_u$ state having few vibrational levels that tend to be blended with other electronic state v levels. Regardless, the present ICSs better describe the excitation function shape compared to other works.

The ICS values of Trajmar *et al.* [16] appear to be too small versus the present ICSs (∼2.5 times at ∼50 eV), which do not agree within the experimental uncertainties. It is curious that Chutjian *et al.* [44] (the source for Ref. [16]) show fewer data points and a longer "dashed segment" (i.e., representing nonmeasured, estimated data) for the $o_3\ ^1\Pi_u$ state than the other dipole-allowed states (see their Figs. 4 and 6), possibly suggesting unfolding issues with subsequent interpolation and/or extrapolation of the DCSs affecting their ICSs. Further, details regarding the vibrational contribution of their ICSs are not clearly stated, though it appears that this includes $v' =$ 0–4. As discussed in Khakoo *et al.* [34], DCSs (ICSs) of the $o_3\ ^1\Pi_u$ state are relatively susceptible to inaccuracies through the unfolding of the EEL spectra due to weak and overlapped vibrational intensities. This was also apparent in the recent work of Heays *et al.* [49], which, combined with the present work, suggests a similar ICS shape for both the $3p\pi_u\ c_3\ ^1\Pi_u$ and $3s\sigma_g\ o_3\ ^1\Pi_u$ Rydberg states, or at least a shape different than that of the $b\ ^1\Pi_u$ state ICS.

Also shown in Fig. 3 is the recent excitation cross-section value of Ajello *et al.* [2], which is a reevaluation of previous emission and predissociation data by Ajello and coworkers (see James *et al.* [36], Table 6). We note that no change was made by Ajello *et al.* [2] to the original $o_3\ ^1\Pi_u$ ($v' = 0$–5) state cross section tabulated by James *et al.* [36], nor have we provided a renormalization of this in the present work. The cross section of Ajello *et al.* [2] is larger than the present 100-eV data by a factor of ∼1.4, though still within the *shared* experimental uncertainties. Also, intensity attributable to the $v' = 5$ level is negligible [72] compared to the difference in cross-section values. The assumption of negligible cascade to the $o_3\ ^1\Pi_u$ state from, for instance, the $y\ ^1\Pi_g$ and $x\ ^1\Sigma_g^-$ states, is reasonable based on the results of Allen *et al.* [87]. It was noted in Ref. [87] that the $x\ ^1\Sigma_g^-$ state is more likely to radiate to the $a'\ ^1\Sigma_u^-$ state rather than the $o_3\ ^1\Pi_u$ state, while the $y\ ^1\Pi_g$ state is more likely to transition to the $w\ ^1\Delta_u$ and $a'\ ^1\Sigma_u^-$ states rather than the $o_3\ ^1\Pi_u$ and $c_4'\ ^1\Sigma_u^+$ states. Further, Ajello *et al.* [2] (and James *et al.* [36]) stated a predissociation of 100% (similar to Zipf and McLaughlin [71]) for the $o_3\ ^1\Pi_u$ state, which was based on their observed emissions and the results of Geiger and Schröder [53] (see the discussion in Sec. IV A). This could contribute to the disagreement between the present ICSs compared with the $o_3\ ^1\Pi_u$ cross section of Ajello *et al.* [2].

Allen *et al.* [87] measured emission cross sections for the $o_3\ ^1\Pi_u$ ($v' = 0$) → $a\ ^1\Pi_g$ ($v' = 0$) transition as a function of E_0 and reported at 75 eV (i.e., the intensity maximum) an absolute value of $(0.40 \pm 0.15) \times 10^{-21}$ cm^2. As shown in Fig. 3, the optical emission of Allen *et al.* has a shape (intensity was arbitrarily scaled), as a function of E_0, consistent with the present ICSs. It is also curious that $o_3\ ^1\Pi_u \rightarrow a\ ^1\Pi_g$ emission was observed in Ref. [87] while $o_3\ ^1\Pi_u \rightarrow X\ ^1\Sigma_g^+$ emission was not reported by Ajello and co-workers [2,36,74]: The former requires two active electrons (noting the configurations $(1\pi_u)^3(3\sigma_g)^2\ 3s\sigma_g\ o_3\ ^1\Pi_u$ and $(1\pi_u)^4(3\sigma_g)^1(1\pi_g)^1\ a\ ^1\Pi_g$ [35]) while the latter requires one electron (i.e., $3s\sigma_g \rightarrow 1\pi_u$ [35]) and is dipole allowed. [Of note, Morgan and Mentall [84] claimed to have observed $o_3\ ^1\Pi_u \rightarrow X\ ^1\Sigma_g^+$ emissions, specifically $o_3(0,0)$ and $o_3(0,2)$ at 200 eV, but their spectral resolution and previously discussed experimental issues are causes of concern whereby their observations need confirmation. However, Roncin *et al.* [37] observed $o_3(v' = 0$–$4) \rightarrow X(v'')$ emissions in a discharge and Ajello [89] suggests various $o_3(v',v'')$ emissions were observed in recent work.] Even though the $o_3(0) \rightarrow a(0)$ transition is very weak, the observed emission stemming from the $o_3\ ^1\Pi_u$ state indicates that the predissociation amount (100%) used by emission-based excitation cross-section estimations of the $o_3\ ^1\Pi_u$ state (e.g., Ajello *et al.* [2]) may need adjustment, with a corresponding revision to the excitation values.

D. The $b'\ ^1\Sigma_u^+$ state

The present ICSs of the $b'\ ^1\Sigma_u^+$ state, listed in Table II, were limited to $v' = 0$–10 due to the range of the unfolded EEL data (up to 13.82 eV) [34]. This partial (measured) contribution amounted to less than 10% of the excitation cross section (see the REP values in Table I). A significant amount of the $b'\ ^1\Sigma_u^+$ state cross-section intensity is due to excitation of the $v' =$ 14–17 levels [72,74]. The $b'\ ^1\Sigma_u^+$ state of N_2 has at least 41 discrete vibrational levels based on the photoabsorption study of Huber and Jungen [90]. Further, the sum of "effective FCFs" for the $v' = 0$ to $v' = 28$ levels given by Stahel *et al.* [72] (based on their Tables VIII and IX) is 0.9946. In contrast, the sum of effective FCFs [72] of the $v' = 0$–10 and $v' =$ 0–18 levels is 0.0830 and 0.7376 (see below), respectively. Consequently, most of the intensity of the $b'\ ^1\Sigma_u^+$ state was unfortunately missed in the DCS work of Khakoo *et al.* [34], and consequently in the present ICS work, to such an extent that we have only included some "full" $b'\ ^1\Sigma_u^+$ state ICS results in Table III and in Fig. 4 (see below for methodology).

Mu-Tao and McKoy [48], Hazi [62], and Chung and Lin [61] have used theoretical calculations to generate excitation cross sections for the $X\ ^1\Sigma_g^+ \rightarrow b'\ ^1\Sigma_u^+$ transition. The $b'\ ^1\Sigma_u^+$ state ICSs of Trajmar *et al.* [16], presumably covering $v' =$ 0–16 (certainly $v' < 16$, based on Figs. 1–3 of Chutjian *et al.* [44]), appear to indicate too rapid of a falloff. Mu-Tao and McKoy [48] apparently covered the $v' = 0$–16 range since they utilized the measured relative intensities of Geiger and Schröder [53] to handle perturbations over the 12.9–14.2 eV EEL range, which was approximately the same upper EEL value as Trajmar *et al.* [16]. Since the $b'\ ^1\Sigma_u^+$ state ICSs of Trajmar *et al.* [16] and Mu-Tao and McKoy [48] only covered a subset of v' levels, they represent lower limits to the "full" ICSs.

The present partial ICSs may be scaled upward by a factor of ∼2.75 to account for unmeasured vibronic transitions. This scaling factor is the approximate factor required to account for the separation between the DCSs of Khakoo *et al.* [34] and the $b'\ ^1\Sigma_u^+$ state results of Mu-Tao and McKoy [48] near ∼90° (see Sec. IV E, as well as Fig. 7 in Ref. [34], for further details). The present $b'\ ^1\Sigma_u^+$ state full-ICS estimations presented in Table III were determined in this manner. Note, this scaling to a full-state ICS (equivalent presumably to the

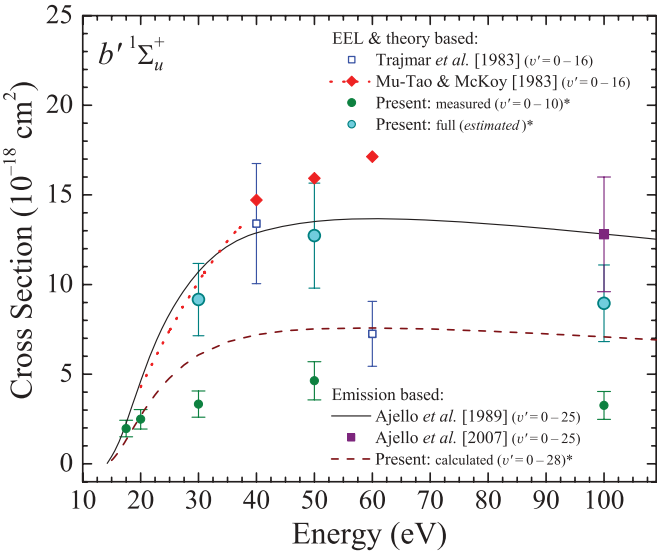

FIG. 4. (Color online) Cross sections for electron-impact excitation of the $b'\ ^1\Sigma_u^+$ state in N_2. The asterisk (*) in the figure legend brings attention to the present full-ICS *estimations* ($v' = 0$–16 equivalence) and the present calculated excitation cross section ($v' =$ 0–28), which were determined as explained in Sec. IV D. While the thermally averaged CSE-calculated OOS used in normalizing the present calculated cross section is accurate, the collision strength parameters of Ajello *et al.* [74] are in question, as discussed in the text.

$v' = 0$–16 levels) is admittedly *ad hoc* with difficult to estimate uncertainties associated. As such, the errors quoted in Table III only represent the experimental errors common to the other partial-state (measured) ICS determinations (see Table II) and do not include a representative error associated with the scaling procedure. However, full-ICS estimations are only given at 30, 50, and 100 eV since the Mu-Tao and McKoy [48] results, which are given at 40 and 60 eV, are insufficient to guide and/or constrain scaling of the present partial-ICS data at 17.5 and 20 eV. Also, since the present partial-ICSs are made full by scaling the Khakoo *et al.* [34] partial DCS to the Mu-Tao and McKoy [48] DCS in the vicinity of 90°, the fact that the Mu-Tao and McKoy ICS is noticeably larger than the present full ICS (and other excitation shapes) suggests their DCSs may be overestimated for $\theta \rightarrow 0^\circ$ (which also appears to be the case for the $c_4'\ ^1\Sigma_u^+$ state) even though the overall DCS shape agreement is good. This estimation method implicitly assumes the overall DCSs of Mu-Tao and McKoy [48] are of approximately correct absolute magnitude. Interestingly, these present full and scaled ICSs have reasonable agreement with other data sets.

Ajello *et al.* [74] determined a set of collision strength parameters from a fit of the measured relative emission intensities of the $b'\ ^1\Sigma_u^+$ ($v' = 16$) $\rightarrow$ $X\ ^1\Sigma_g^+$ ($v'' = 0$) band (at 87.14 nm) with E_0 values from 14.23 to 400 eV. The "accuracy of the fit" was claimed to be better than 5%. Curiously, the $b'\ ^1\Sigma_u^+$ state cross-section determination was *not* made absolute using the relative flow method as they did for the cross section of the $c_4'\ ^1\Sigma_u^+$ state in their same publication (see Sec. IV E). Instead, Ajello *et al.* [74] obtained individual vibrational band OOSs by using their calculated FCFs (lacking details) and an OOS of 0.321 (see the discussion near Table VI of Ref. [74]) for the $b'\ ^1\Sigma_u^+ \rightarrow X\ ^1\Sigma_g^+$ band system. The calculated FCFs are (expectedly) not in agreement with the work of Stahel *et al.* [72], as well as the CSE results, and are thus an additional source of inaccuracy not accounted for in their quoted uncertainty. The collision strength parameters, along with the derived vibrational band OOSs, produce the vibrational band cross sections over a range of excitation energies. Figure 4 indicates reasonable agreement with the present *estimated* full and scaled ICS and the emission-based $b'\ ^1\Sigma_u^+$ ($v' = 0$–25) excitation cross section of Ajello *et al.* [74], though we note the large uncertainty in the present estimation.

However, there are two significant problems in the $b'\ ^1\Sigma_u^+ \rightarrow X\ ^1\Sigma_g^+$ cross sections of Ajello *et al.* [74]. First, the relative cross sections calculated from the collision strength parameters in their Table VII(b) actually differ very significantly from those listed in their Table VI. Between 20 and 40 eV, the calculated relative cross sections are ~8–32% greater than those listed in their Table VI. These differences are much larger than the <5% error claimed. Second, even if the derived $b'\ ^1\Sigma_u^+ \rightarrow X\ ^1\Sigma_g^+$ collision strength parameters were accurate, the excitation cross sections listed in their Table VII(b) are significantly overestimated because the vibrational band OOSs used by Ajello *et al.* [74] are generally much larger than those recently measured by Heays *et al.* [73] using a more accurate high-resolution photoabsorption technique.

Reevaluation of the original $b'\ ^1\Sigma_u^+$ ($v' = 0$–25) state cross section, tabulated by James *et al.* [36] (see their Table 6, based on the emission work of Ref. [74]), was provided by Ajello *et al.* [2], where the previous emission and predissociation data was adjusted (see their discussion). The emission cross section of Ajello *et al.* [74] is 28.4% larger than Ajello *et al.* [2]; the predissociation cross section of Ajello *et al.* [2] was increased by 4.2% compared to Ref. [74]. Further, while keeping the resultant excitation cross section the same, the predissociation rate was changed from 84.4% to 87.9%.

The present calculation (emission based) of the excitation cross section for the $b'\ ^1\Sigma_u^+$ ($v' = 16$) level at 100 eV, based on the collision strength parameter of Ajello *et al.* [74] and the CSE OOS [73], is 1.18×10^{-18} cm^2. This value is less than the 2.67×10^{-18} cm^2 cross section obtained by Ajello *et al.* [74]. In addition to the inconsistency in the relative cross section of the $b'\ ^1\Sigma_u^+$ ($v' = 16$) level noted earlier, the optical depths and self-absorption were also incorrectly estimated by Ajello *et al.* [74]. In their analysis, they treated the $J'' = 7$ level as if it were the most populated level of the ground state, $X\ ^1\Sigma_g^+$ ($v' = 0, J''$), when, in fact, it is not even among the top five most populated levels at 300 K. (The strong rotational dependence of the OOS also requires caution when using band OOSs to estimate optical depths.) Thus, in the present work, the $b'\ ^1\Sigma_u^+$ state calculated excitation cross section was obtained with the collision strength parameters of Ajello *et al.* [74] and the CSE calculated P- and R-branch OOSs (which are essentially the measured values of Stark *et al.* [5], Heays *et al.* [73], and Heays [91]) for the $v' = 0$–28 levels. Figure 4 shows the present (emission-based) calculated excitation cross section of the $X\ ^1\Sigma_g^+$ ($v' = 0$) – $b'\ ^1\Sigma_u^+$ ($v' = 0$–28) transition. The large difference between the present calculated cross section and the Ajello *et al.* [74] cross section is primarily due the difference in the (near-full) band OOS: Ajello *et al.* [74]

used an OOS of 0.321 for the $v' = 0$–25 levels, while the "whole electronic band" OOS (*less than* 0.321) is used in the present work. [Note: The 0.239 estimated CSE OOS value, as reported by Khakoo *et al.* [34] (see their Table IV), is supplanted by the more accurate method employed in the present work for the thermally averaged, at 300 K, CSE OOS for the essentially whole $X\ ^1\Sigma_g^+$ (0) – $b'\ ^1\Sigma_u^+$ (0–28) electronic band.] The presently utilized OOS is more accurate than that of Ajello *et al.* [74] because it is based on both photoabsorption measurements and CSE calculations. However, the presently calculated estimation of the excitation cross section may be inaccurate *in shape* (and, thus, also in magnitude for low E_0) due to the questionable collision strength parameters of Ajello *et al.* [74].

We also note the emission-based cross-section data of Zipf and McLaughlin [71], which are partly based on the relative intensities of Geiger and Schröder [53] (see the discussion in Sec. IV A), has a renormalized (via N I 120.0 nm from N_2) total ($v' = 0$–20) excitation cross section of 9.44×10^{-18} cm^2 at 200 eV and a stated predissociation branching ratio of 0.83. This is approximately the same as for the renormalized Ajello *et al.* [74] data. Morgan and Mentall [84] measured several $b'\ ^1\Sigma_u^+(v') \rightarrow X\ ^1\Sigma_g^+(v'')$ emissions at 200 eV (see their Table II). As explained above (see Sec. IV A), we suggest caution be applied when using the Morgan and Mentall [84] data.

Therefore, in summary, the $b'\ ^1\Sigma_u^+$ state requires additional measurements to address inconsistencies among numerous data sets in its relative shape *and* absolute excitation cross section.

E. The $c_4'\ ^1\Sigma_u^+$ state

The $c_4'\ ^1\Sigma_u^+$ state excitation cross sections are shown in Fig. 5, with the present values provided in Tables II and III. The present ICSs are shown for both the measured partial ($v' =$ 0–3) and REP-based full ($v' = 0$–8) contributions, where the partial (measured) contribution represents 82.5% of the cross section (see Table I). Also shown in Fig. 5 are the excitation cross sections of Ajello *et al.* [2], Ajello *et al.* [74], Trajmar *et al.* [16], and Mu-Tao and McKoy [48] from near threshold to >100 eV. The $c_4'\ ^1\Sigma_u^+$ ($v' = 0$–7) emission-based excitation cross section of Ajello *et al.* [74] was renormalized via the factor 7.03/7.3 (Lyman-α from H_2 [67,69]). The recently reevaluated excitation cross section of Ajello *et al.* [2] (see their Table 1 and the discussion below) was not renormalized in the present work. The data of Zipf and McLaughlin [71], which are partly based on the relative intensities of Geiger and Schröder [53] (see the discussion in Sec. IV A), are not displayed and has a renormalized (via N I 120.0 nm from N_2) total ($v' = 0$–7) excitation cross section of 13.15×10^{-18} cm^2 at 200 eV and a stated predissociation branching ratio of ~0.15 for $v' = 0$–4 and >0.95 for $v' = 5$–7. This cross-section value is apparently too large and further their predissociation amounts are suspect.

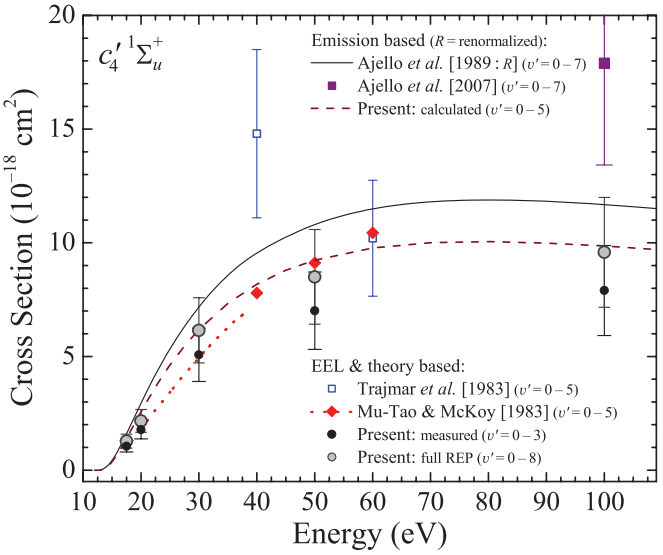

FIG. 5. (Color online) Cross sections for electron-impact excitation of the $c_4'\ ^1\Sigma_u^+$ state in N_2.

The present emission-based estimation to the $c_4'\ ^1\Sigma_u^+$ state excitation cross section, covering $v' = 0$–5 (equivalent to the present "full" ICS), was constructed similar to the method described earlier (i.e., as discussed immediately above Sec. IV A). Figure 5 shows very good agreement between the present emission-based calculation and EEL results. Thus, the EEL data confirms the accuracy of the $c_4'\ ^1\Sigma_u^+$ state excitation function shape and the CSE-optimized OOS. Also, curiously, the $c_4'\ ^1\Sigma_u^+$ state excitation cross section of Ajello *et al.* [74] (see below), for *only* the $v' = 0$–3 levels, agrees with the present calculated $v' = 0$–5 excitation cross section.

The ICSs of Trajmar *et al.* [16] are shown in Fig. 5, noting that the vibrational coverage is not explicitly stated in their paper, but appear to include $v' = 0$–5 (certainly $v' < 5$, based on Figs. 1–3 of Chutjian *et al.* [44]). While the 60-eV ICS appears accurate, their 40-eV ICS is spuriously high and suggests a strange excitation function shape. Also shown in Fig. 5 are the theoretical results of Mu-Tao and McKoy [48]: Early distorted-wave calculations generated DCSs at 40 and 60 eV from 0° to 180°, as well as ICSs between 20 and 60 eV. The measured relative intensities of Geiger and Schröder [53] were used to construct effective FCFs in Ref. [48] to handle perturbations over the 12.9–14.2 eV EEL range (note: 14.2 eV was the approximate upper EEL range of Chutjian *et al.* [44]). This suggests the $c_4'\ ^1\Sigma_u^+$ state excitation cross section of Mu-Tao and McKoy [48] includes the $v' = 0$–5 (certainly $v' < 5$) contributions.

For comparison convenience, we constructed a 50-eV DCS from an unweighted average of the 40- and 60-eV DCSs of Mu-Tao and McKoy [48], which was shown to be in excellent agreement with the $c_4'\ ^1\Sigma_u^+$ state DCSs of Khakoo *et al.* [34] (see their Fig. 7). These three DCSs were integrated over the entire 0°–180° scattering angular range to generate corresponding ICSs. The ICSs shown in Ref. [48] had a slightly strange shape (at least when digitizing the data curve), disagreeing with the DCS-generated ICSs above roughly 38 eV, and is only shown up to this E_0 value in Fig. 5. Overall, the ICSs of Mu-Tao and McKoy [48] agree well with the present ICSs within experimental uncertainty.

Figure 5 illustrates the disagreement (beyond uncertainties) in the cross section of Ajello *et al.* [2] with both the present ICSs and the present emission-based estimation of the

excitation cross section, as well as other previously published data. Ajello *et al*. [2] (see their Table 1) reevaluated previous emission and predissociation data by Ajello and co-workers: They included a revised $c_4'\ ^1\Sigma_u^+$ ($v'=0$) excitation cross section with nonzero predissociation; predissociation was included for the $v'=3$–4 levels based on their $c_4'\ ^1\Sigma_u^+$ state addendum work [92]; temperature-dependent predissociation was included for the $c_4'\ ^1\Sigma_u^+$ ($v'=0$) state based on the work of Liu *et al*. [93]; and additional $c_4'\ ^1\Sigma_u^+$ ($v'=0$) – $X\ ^1\Sigma_g^+$ ($v''=6$–12) bands were incorrectly included based on the atmospheric observations of Bishop *et al*. [94]. Regardless of these "corrections," the significant excitation cross-section dissimilarity with the present work, and other works, suggests an error might have been incurred in the course of their reanalysis.

The Ajello *et al*. [74] excitation shape function, from threshold to >100 eV, for the $c_4'\ ^1\Sigma_u^+$ ($v'=0$–7) state was constructed using their published parameters (see their Table VII) for the modified Born approximation [81,82]. This was scaled using their renormalized 100-eV cross-section data point, which they originally made absolute using the relative flow method and comparison to prominent atomic emission lines (e.g., N I 120.0 nm from N_2 and H I 121.6 nm Lyman-α from H_2). We note that they also reported lower cross-section values (up to ∼20% less) when using OOSs (or lifetimes and branching ratios) and the modified Born approximation for absolute normalization. The $c_4'\ ^1\Sigma_u^+$ ($v'=0$) → $X\ ^1\Sigma_g^+$ ($v''=0$) emission intensity (at 95.8 nm) as a function of E_0 was the basis for their excitation function shape. The assumption of negligible cascade to the $c_4'\ ^1\Sigma_u^+$ state from, e.g., the $y\ ^1\Pi_g$ state, is deemed reasonable based on the results of Allen *et al*. [87], where it was noted that the $y\ ^1\Pi_g$ state is more likely to transition to the $w\ ^1\Delta_u$ and $a'\ ^1\Sigma_u^-$ states rather than the $c_4'\ ^1\Sigma_u^+$ and $o_3\ ^1\Pi_u$ states. Also, branching to the $a\ ^1\Pi_g$ state appears to be negligible (even more so for the possible $c_4'\ ^1\Sigma_u^+ \rightarrow a''\ ^1\Sigma_g^+$ transition) compared to the $c_4'\ ^1\Sigma_u^+ \rightarrow X\ ^1\Sigma_g^+$ transition probability [88,95–97]. (A recent 25- and 100-eV electron-impact emissions investigation, between 330 and 1100 nm, by Ajello and co-workers [98] unfortunately overlooked potential $c_4'\ ^1\Sigma_u^+ \rightarrow a\ ^1\Pi_g$ emissions.) However, there is cause for concern due to the relative flow normalization method being used in Ref. [74] instead of accurate OOSs. We also note the relatively large difference in wavelength between the 95.8- and ∼120-nm emissions, which might affect normalization procedures with regard to the optical transmission of the spectrometers used. This applies to the emission intensity determinations (at 100 eV) of numerous vibronic features across an expanded wavelength range, which was used to construct their entire $c_4'\ ^1\Sigma_u^+$ ($v'=0$–7) emission-based excitation cross section. This also was vulnerable to inaccuracies from blending with other unresolved emission features and difficult-to-partition intensities into particular spectral components (see Sec. IV A). The relative sensitivity of the optical detection system was susceptible to inaccuracies, especially below ∼95 nm, due to the optical sensitivity calibration technique: Their early $e^- + H_2$ model (i.e., before ∼1995) did not adequately account for emission from the $B'\ ^1\Sigma_u^+$, $D\ ^1\Pi_u$, and higher states. Furthermore, a major flaw in their analysis of the $c_4'\ ^1\Sigma_u^+$ state was in using a zero predissociation amount for the transition corresponding to the 95.8-nm emission. This is somewhat inconsistent considering, for instance, the previous work of Zipf and McLaughlin [71] had determined a nonzero predissociation fraction. Nevertheless, the emission-based excitation cross section of Ajello *et al*. [74] remains in reasonable agreement (within uncertainties) with the present excitation cross sections, unlike the revised value of Ajello *et al*. [2].

The $c_4'(0) - X(0)$ transition

The $X\ ^1\Sigma_g^+$ ($v'=0$) – $c_4'\ ^1\Sigma_u^+$ ($v'=0$) transition is the strongest feature in the investigated EEL range of N_2 and its corresponding emission is one of the strongest features under optically thin conditions. Figure 6 shows excitation cross sections for the $c_4'\ ^1\Sigma_u^+$ (0) state with data sets stemming from the discussion pertaining to Fig. 5. The present $c_4'\ ^1\Sigma_u^+$ (0) ICS was established using the $c_4'\ ^1\Sigma_u^+$ ($v'=0$–7) ICS adjusted by the REP value of 0.785 ± 0.025 (see Table I). The presently calculated emission-based estimation to the excitation cross section was constructed as explained above, but for only the $v'=0$ level. The present ICS and calculated excitation cross section are in excellent agreement.

The excitation function of Ajello *et al*. [74] was constructed as in Fig. 5 using the $c_4'\ ^1\Sigma_u^+$ ($v'=0$) → $X\ ^1\Sigma_g^+$ ($v''=0$) emission intensity made absolute using the relative flow method and renormalized in this work via the factor 7.03/7.3 (Lyman-α from H_2 [67,69]). There is good agreement between the present excitation cross sections and the emission-based excitation cross section of Ref. [74]. The main shortcoming of the Ajello *et al*. [74] "optically thin" result was the assumed 100% emission yield, though predissociation is certainly known to be nonzero. Note that in order to obtain the excitation cross section to the $c_4'\ ^1\Sigma_u^+$ (0) state, they had to use the emission branching ratio or the summation of the measured emission cross sections, $\sigma_{em}(v') = \Sigma_{v''}\sigma_{em}(v',v'')$, for $c_4'\ ^1\Sigma_u^+$ ($v'=0$) → $X\ ^1\Sigma_g^+$ (v'') over sufficient v'', but unfortunately not all v''. Moreover, the effect of the coupling between the

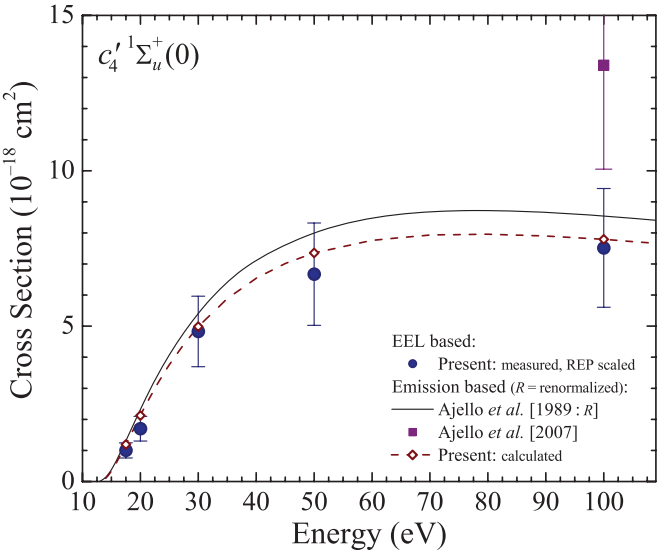

FIG. 6. (Color online) Cross sections for electron-impact excitation of the $c_4'\ ^1\Sigma_u^+$ ($v'=0$) state in N_2.

$b\,^1\Pi_u$ (1) and $c_4'\,^1\Sigma_u^+$ (0) states on the branching ratio was not taken into account by Ajello *et al.* [74].

Ajello *et al.* [2] provided a revised $c_4'\,^1\Sigma_u^+$ (0) excitation cross section of 13.4×10^{-18} cm^2 at 100 eV. This value was updated, compared to the published (i.e., prerenormalization) excitation value (12.14×10^{-18} cm^2 at 100 eV) of Ref. [74], via changes to the emission and predissociation cross sections. Specifically, additional $v'' = 6$–12 bands were included based on atmospheric observations [94], along with a nonzero predissociation amount that was room-temperature adjusted to 300 K based on Ref. [93]. Again, the significant difference in the excitation cross section of Ajello *et al.* [2], shown in Fig. 6 compared to the other data sets, appears to suggest an error was made in their reanalysis, particularly with the $c_4'\,^1\Sigma_u^+$ (0) state and converting from emission to excitation.

Morgan and Mentall [84] also measured the $c_4'\,^1\Sigma_u^+$ ($v' = 0$) $\rightarrow$ $X\,^1\Sigma_g^+$ ($v'' = 0$) emission intensity (at 95.8 nm) at an E_0 value of 200 eV, as well as several other $c_4'(v',v'')$ emissions. As explained above (see Sec. IV A), caution is warranted for the Morgan and Mentall [84] data, though a renormalization (7.03/12.3 for Lyman-α from H_2 [67,86]) provides an adjusted *emission* cross section of 2.93×10^{-18} cm^2 at 200 eV for $c_4'(0,0)$. This value appears to be too low even after adjusting for predissociation. Other emission-based measurements were by Becker *et al.* [99], who looked at rotational envelope effects at various E_0 values, as well as the polarization and excitation-function work of Huschilt *et al.* [100]. [Of note: An old measurement of the $c_4'(0,1)$ emission cross section, previously identified as the legacy $p'\,^1\Sigma_u^+$ (0,1) emission, was made by Aarts and de Heer [97].] It was found that the polarization, for the $c_4'(0,0)$ and $c_4'(0,1)$ emissions, converged to zero as E_0 increased to ~120–150 eV. Also, Huschilt *et al.* [100] measured a relative emission cross section for $c_4'(0,0)$ (with an absolute value of 8.1×10^{-18} cm^2 at 100 eV, as normalized to the 150 eV theoretical ICS of Hazi [62]), which has a shape comparable to that of the present work for roughly $E_0 > 30$ eV.

F. The $G\,^3\Pi_u$, $F\,^3\Pi_u$, and $D\,^3\Sigma_u^+$ states

Table II lists the present ICSs of the $G\,^3\Pi_u$ and $F\,^3\Pi_u$ states that are shown in Figs. 7 and 8, respectively, and represent essentially the "full" ($v' = 0$–3) vibrational contributions (see Khakoo *et al.* [34] for details). The $D\,^3\Sigma_u^+$ state was briefly discussed in Khakoo *et al.* [34] as being too weak to reliably unfold relative to the other contributions in the EEL spectra, which indicated a negligible DCS (probably on the order of 10^{-21} cm^2 sr^{-1}) with a correspondingly small ICS (~10^{-20} cm^2). This negligibly small cross-section result was also noted by Chutjian *et al.* [44] at the studied incident energies. Furthermore, *emissions* from the $D\,^3\Sigma_u^+$ state (which may include cascade contributions) have been studied by Filippelli *et al.* [88,101] (and references therein, where the emission study of Freund [102] was only relative), indicating a somewhat larger cross section of approximately 1×10^{-19} cm^2 at about 20 eV with a quick decrease with increasing energy. This is reasonably consistent with the present results.

The ICSs of Trajmar *et al.* [16], which are a renormalization of the Chutjian *et al.* [44] data, are the only other (integral) excitation cross sections that we are aware of for the $G\,^3\Pi_u$ and $F\,^3\Pi_u$ states. Specifically, the vibrational coverage of Trajmar *et al.* [16] appears to have included $v' = 0$–1 for the $G\,^3\Pi_u$ state and $v' = 0$–3 for the $F\,^3\Pi_u$ state. The $G\,^3\Pi_u$ state ICS of Trajmar *et al.* [16] did not cover the same v'-level range ($v' = 0$–3) as the present, thus it is a lower limit to their "full" ICS. Khakoo *et al.* [34] indicated a significantly smaller "backscatter" contribution for $\theta > 70°$ compared to the DCSs of Trajmar *et al.* [16]. This probably accounts for the differences between ICSs shown in Figs. 7 and 8, which both indicate larger ICSs for Trajmar *et al.* [16] versus the present data (~1.5 times larger at ~50 eV), though agreement just within the range of uncertainties is apparent. As discussed in Khakoo *et al.* [34], the shapes of their DCSs, which the present ICSs are based on, are typical of forbidden excitations. Figures 7 and 8 both support this observation with

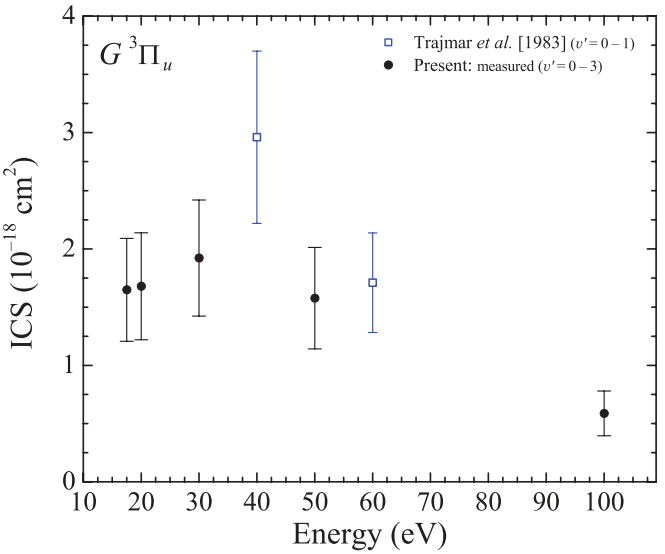

FIG. 7. (Color online) ICSs for electron-impact excitation of the $G\,^3\Pi_u$ state in N_2.

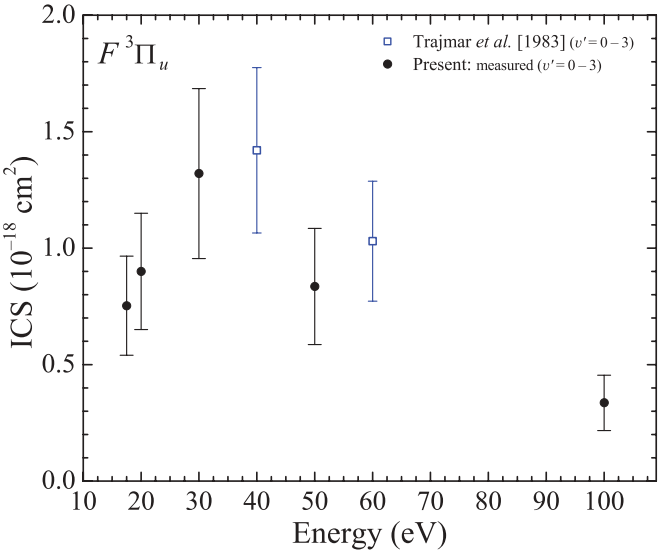

FIG. 8. (Color online) ICSs for electron-impact excitation of the $F\,^3\Pi_u$ state in N_2.

the excitation functions indicating a rapid increase to peak and reasonably quick falloff in intensity.

V. CONCLUSIONS

Integral cross sections are reported for electron-impact direct excitation of the $b\,^1\Pi_u$, $c_3\,^1\Pi_u$, $o_3\,^1\Pi_u$, $b'\,^1\Sigma_u^+$, $c_4'\,^1\Sigma_u^+$, $G\,^3\Pi_u$, and $F\,^3\Pi_u$ electronic states out of the ground-state level $X\,^1\Sigma_g^+$ ($v' = 0$) in N_2. These were obtained at incident energies of 17.5, 20, 30, 50, and 100 eV based on the DCSs of Khakoo *et al*. [34] in the ∼12–13.82 eV unfolded EEL range and for scattering angles ranging from 2° to 130°. We have compared the present cross sections with available EEL-based measurements, theoretical calculations, and emission-based work: We generally find good agreement within error estimations with available results, except with the recent reevaluation provided by Ajello *et al*. [2]. The excitation cross sections of states that heavily predissociate, such as the $c_3\,^1\Pi_u$ and $o_3\,^1\Pi_u$ states, evident by CSE and emission studies, are effectively partial cross sections for production of dissociative N. Future EEL work should include the unfolding of better resolved features above ∼13.82 eV as well as DCSs at larger scattering angles to verify the presently utilized DCS extrapolations. Future optical emission work should include remeasurements of excitation shape functions of the singlet *ungerade* states utilizing better spectral resolution than past determinations (e.g., Ajello *et al*. [74] and James *et al*. [36]) to avoid uncertainties associated with unresolved and/or blended spectral features and J-dependent predissociation. Further development of theoretical treatments of N_2 excitation is also in need.

ACKNOWLEDGMENTS

This work was performed at the California State University, Fullerton (CSUF) and at the Jet Propulsion Laboratory (JPL), California Institute of Technology (Caltech), under a contract with the National Aeronautics and Space Administration (NASA). We gratefully acknowledge financial support through NASA's Outer Planets Research (OPR) and Planetary Atmospheres (PATM) programs and the National Science Foundation, under Grants No. NSF-AGS-0938223, No. NSF-PHY-RUI-0096808, and No. NSF-PHY-RUI-0965793. We are grateful to Dr. B. R. Lewis and Dr. A. N. Heays for supplying data prior to publication.

[1] J. M. Ajello, J. Gustin, I. Stewart, K. Larsen, L. Esposito, W. Pryor, W. McClintock, M. H. Stevens, C. P. Malone, and D. Dziczek, Geophys. Res. Lett. **35**, 5 (2008).
[2] J. M. Ajello, M. H. Stevens, I. Stewart, K. Larsen, L. Esposito, J. Colwell, W. McClintock, G. Holsclaw, J. Gustin, and W. Pryor, Geophys. Res. Lett. **34**, L24204 (2007).
[3] M. H. Stevens, J. Gustin, J. M. Ajello *et al*., J. Geophys. Res., [Space Phys.] **116**, A05304 (2011).
[4] S. A. Stern, D. C. Slater, J. Scherrer *et al*., Space Sci. Rev. **140**, 155 (2008).
[5] G. Stark, B. R. Lewis, A. N. Heays, K. Yoshino, P. L. Smith, and K. Ito, J. Chem. Phys. **128**, 114302 (2008).
[6] M. O. Vieitez, T. I. Ivanov, C. A. de Lange, W. Ubachs, A. N. Heays, B. R. Lewis, and G. Stark, J. Chem. Phys. **128**, 11 (2008).
[7] X. Liu, D. E. Shemansky, C. P. Malone, J. M. Ajello, I. Kanik, A. N. Heays, B. R. Lewis, S. T. Gibson, and G. Stark, J. Geophys. Res., [Space Phys.] **113**, A02304 (2008).
[8] G. Stark, K. P. Huber, K. Yoshino, P. L. Smith, and K. Ito, J. Chem. Phys. **123**, 214303 (2005).
[9] P. V. Johnson, C. P. Malone, I. Kanik, K. Tran, and M. A. Khakoo, J. Geophys. Res., [Space Phys.] **110**, A11311 (2005).
[10] M. A. Khakoo, P. V. Johnson, I. Ozkay, P. Yan, S. Trajmar, and I. Kanik, Phys. Rev. A **71**, 062703 (2005).
[11] C. P. Malone, P. V. Johnson, I. Kanik, B. Ajdari, and M. A. Khakoo, Phys. Rev. A **79**, 032704 (2009).
[12] C. P. Malone, P. V. Johnson, J. A. Young, X. Liu, B. Ajdari, M. A. Khakoo, and I. Kanik, J. Phys. B **42**, 225202 (2009).
[13] M. A. Khakoo, S. Wang, R. Laher, P. V. Johnson, C. P. Malone, and I. Kanik, J. Phys. B **40**, F167 (2007).
[14] L. Campbell, M. J. Brunger, A. M. Nolan, L. J. Kelly, A. B. Wedding, J. Harrison, P. J. O. Teubner, D. C. Cartwright, and B. McLaughlin, J. Phys. B **34**, 1185 (2001).
[15] D. C. Cartwright, S. Trajmar, A. Chutjian, and W. Williams, Phys. Rev. A **16**, 1041 (1977).
[16] S. Trajmar, D. F. Register, and A. Chutjian, Phys. Rep. **97**, 219 (1983).
[17] R. F. da Costa and M. A. P. Lima, Int. J. Quantum Chem. **106**, 2664 (2006).
[18] R. F. da Costa and M. A. P. Lima, Phys. Rev. A **75**, 022705 (2007).
[19] M. Tashiro and K. Morokuma, Phys. Rev. A **75**, 012720 (2007).
[20] H. Kato, D. Suzuki, M. Ohkawa, M. Hoshino, H. Tanaka, L. Campbell, and M. J. Brunger, Phys. Rev. A **81**, 042717 (2010).
[21] J. A. Young, C. P. Malone, P. V. Johnson, J. M. Ajello, X. Liu, and I. Kanik, J. Phys. B **43**, 135201 (2010).
[22] J. M. Ajello and D. E. Shemansky, J. Geophys. Res., [Space Phys.] **90**, 9845 (1985).
[23] J. L. Lean, T. N. Woods, F. G. Eparvier, R. R. Meier, D. J. Strickland, J. T. Correira, and J. S. Evans, J. Geophys. Res., [Space Phys.] **116**, A01102 (2011).
[24] C. P. Malone, P. V. Johnson, I. Kanik, B. Ajdari, S. S. Rahman, S. S. Bata, A. Emigh, and M. A. Khakoo, Phys. Rev. A **79**, 032705 (2009).
[25] P. V. Johnson, J. A. Young, C. P. Malone, M. A. Khakoo, X. Liu, and I. Kanik, J. Phys.: Conf. Ser. **204**, 012003 (2010).
[26] C. P. Malone, P. V. Johnson, J. A. Young, I. Kanik, B. Ajdari, and M. A. Khakoo, J. Phys.: Conf. Ser. **194**, 052020 (2009).
[27] D. E. Shemansky and X. Liu, J. Geophys. Res., [Space Phys.] **110**, A07307 (2005).

[28] D. E. Shemansky, J. M. Ajello, and I. Kanik, Astrophys. J. **452**, 472 (1995).
[29] C. Y. R. Wu, H. S. Fung, K. Y. Chang, and D. L. Judge, Planet Space Sci. **56**, 1725 (2008).
[30] C. Y. R. Wu, H. S. Fung, K. Y. Chang, T. S. Singh, X. L. Mu, J. B. Nee, S. Y. Chiang, and D. L. Judge, J. Chem. Phys. **127**, 084314 (2007).
[31] C. Y. R. Wu, J. I. Lo, Y. C. Lin, H. S. Fung, Y. Y. Lee, T. S. Yih, and D. L. Judge, J. Electron Spectrosc. Relat. Phenom. **184**, 149 (2011).
[32] A. Moise, K. C. Prince, and R. Richter, J. Chem. Phys. **134**, 114312 (2011).
[33] C. Y. R. Wu, D. L. Judge, M. H. Tsai *et al*., J. Chem. Phys. **136**, 044301 (2012).
[34] M. A. Khakoo, C. P. Malone, P. V. Johnson, B. R. Lewis, R. Laher, S. Wang, V. Swaminathan, D. Nuyujukian, and I. Kanik, Phys. Rev. A **77**, 012704 (2008).
[35] A. Lofthus and P. H. Krupenie, J. Phys. Chem. Ref. Data **6**, 113 (1977).
[36] G. K. James, J. M. Ajello, B. Franklin, and D. E. Shemansky, J. Phys. B **23**, 2055 (1990).
[37] J. Y. Roncin, J. L. Subtil, and F. Launay, J. Mol. Spectrosc. **188**, 128 (1998).
[38] J. Y. Roncin and F. Launay, Astron. Astrophys. Suppl. Ser. **128**, 361 (1998).
[39] J. Y. Roncin, F. Launay, H. Bredohl, and I. Dubois, J. Mol. Spectrosc. **194**, 243 (1999).
[40] Y. Itikawa, J. Phys. Chem. Ref. Data **35**, 31 (2006).
[41] Y. Itikawa, M. Hayaski, A. Ichimura, K. Onda, K. Sakimoto, K. Takayanagi, M. Nakamura, H. Nishimura, and T. Takayanagi, J. Phys. Chem. Ref. Data **15**, 985 (1986).
[42] T. Majeed and D. J. Strickland, J. Phys. Chem. Ref. Data **26**, 335 (1997).
[43] T. Tabata, T. Shirai, M. Sataka, and H. Kubo, Atom. Data Nucl. Data Tables **92**, 375 (2006).
[44] A. Chutjian, D. C. Cartwright, and S. Trajmar, Phys. Rev. A **16**, 1052 (1977).
[45] D. C. Cartwright, A. Chutjian, S. Trajmar, and W. Williams, Phys. Rev. A **16**, 1013 (1977).
[46] J. M. Ratliff, G. K. James, S. Trajmar, J. M. Ajello, and D. E. Shemansky, J. Geophys. Res., [Planets] **96**, 17559 (1991).
[47] D. B. Jones, L. Campbell, M. J. Bottema, P. J. O. Teubner, D. C. Cartwright, W. R. Newell, and M. J. Brunger, Planet Space Sci. **54**, 45 (2006).
[48] Lee Mu-Tao and V. McKoy, Phys. Rev. A **28**, 697 (1983).
[49] A. N. Heays, B. R. Lewis, S. T. Gibson, C. P. Malone, P. V. Johnson, I. Kanik, and M. A. Khakoo, Phys. Rev. A **85**, 012705 (2012).
[50] T. J. Whang, G. X. Zhao, W. C. Stwalley, and C. Y. R. Wu, J. Quant. Spectrosc. Radiat. Transfer **55**, 335 (1996).
[51] M. J. Brunger and P. J. O. Teubner, Phys. Rev. A **41**, 1413 (1990).
[52] J. Wrkich, D. Matthews, I. Kanik, S. Trajmar, and M. A. Khakoo, J. Phys. B **35**, 4695 (2002).
[53] J. Geiger and B. Schröder, J. Chem. Phys. **50**, 7 (1969).
[54] G. Joyez, R. I. Hall, J. Reinhardt, and J. Mazeau, J. Electron. Spectrosc. Relat. Phenom. **2**, 183 (1973).
[55] M. A. Khakoo, K. Keane, C. Campbell, N. Guzman, and K. Hazlett, J. Phys. B **40**, 3601 (2007).
[56] L. R. LeClair and S. Trajmar, J. Phys. B **29**, 5543 (1996).
[57] D. S. Newman, M. Lange, J. Matsumoto, J. C. Lower, and S. J. Buckman, presented at the Gaseous Electronics Conference, 2006, [http://meetings.aps.org/link/BAPS.2006.GEC.LW2.6].
[58] M. Furlan, M. J. Hubinfranskin, J. Delwiche, and J. E. Collin, J. Phys. B **23**, 3023 (1990).
[59] D. G. Wilden, P. J. Hicks, and J. Comer, J. Phys. B **12**, 1579 (1979).
[60] J. Mazeau, R. I. Hall, G. Joyez, M. Landau, and J. Reinhard, J. Phys. B **6**, 873 (1973).
[61] S. Chung and C. C. Lin, Phys. Rev. A **6**, 988 (1972).
[62] A. U. Hazi, Phys. Rev. A **23**, 2232 (1981).
[63] M. J. Brunger and S. J. Buckman, Phys. Rep. **357**, 215 (2002).
[64] Y. Ohmori, M. Shimozuma, and H. Tagashira, J. Phys. D: Appl. Phys. **21**, 724 (1988).
[65] A. V. Phelps and L. C. Pitchford, Phys. Rev. A **31**, 2932 (1985).
[66] L. C. Pitchford and A. V. Phelps, Phys. Rev. A **25**, 540 (1982).
[67] J. W. McConkey, C. P. Malone, P. V. Johnson, C. Winstead, V. McKoy, and I. Kanik, Phys. Rep. **466**, 1 (2008).
[68] P. J. M. van der Burgt, W. B. Westerveld, and J. S. Risley, J. Phys. Chem. Ref. Data **18**, 1757 (1989).
[69] J. M. Ajello, D. E. Shemansky, B. Franklin *et al*., Appl. Opt. **27**, 890 (1988).
[70] C. P. Malone, P. V. Johnson, J. W. McConkey, J. M. Ajello, and I. Kanik, J. Phys. B **41**, 095201 (2008).
[71] E. C. Zipf and R. W. McLaughlin, Planet Space Sci. **26**, 449 (1978).
[72] D. Stahel, M. Leoni, and K. Dressler, J. Chem. Phys. **79**, 2541 (1983).
[73] A. N. Heays, B. R. Lewis, G. Stark, K. Yoshino, P. L. Smith, K. P. Huber, and K. Ito, J. Chem. Phys. **131**, 194308 (2009).
[74] J. M. Ajello, G. K. James, B. O. Franklin, and D. E. Shemansky, Phys. Rev. A **40**, 3524 (1989).
[75] http://www.cfa.harvard.edu/amp/ampdata/cfamols.html.
[76] J. Y. Roncin, F. Launay, J. L. Subtil, and K. Yoshino, Planet Space Sci. **39**, 1301 (1991).
[77] J. Y. Roncin, F. Launay, and K. Yoshino, Planet Space Sci. **35**, 267 (1987).
[78] J. Y. Roncin, F. Launay, and K. Yoshino, J. Mol. Spectrosc. **134**, 390 (1989).
[79] E. C. Zipf and M. R. Gorman, J. Chem. Phys. **73**, 813 (1980).
[80] M. J. Mumma and E. C. Zipf, J. Chem. Phys. **55**, 5582 (1971).
[81] D. E. Shemansky, J. M. Ajello, and D. T. Hall, Astrophys. J. **296**, 765 (1985).
[82] D. E. Shemansky, J. M. Ajello, D. T. Hall, and B. Franklin, Astrophys. J. **296**, 774 (1985).
[83] E. C. Zipf, R. W. McLaughlin, and M. R. Gorman, Planet Space Sci. **27**, 719 (1979).
[84] H. D. Morgan and J. E. Mentall, J. Chem. Phys. **78**, 1747 (1983).
[85] C. P. Malone, P. V. Johnson, J. W. McConkey, and I. Kanik, J. Geophys. Res., [Space Phys.] **113**, A06309 (2008).
[86] M. J. Mumma and E. C. Zipf, J. Chem. Phys. **55**, 1661 (1971).
[87] J. S. Allen, S. Chung, and C. C. Lin, Phys. Rev. A **41**, 1324 (1990).
[88] A. R. Filippelli, S. Chung, and C. C. Lin, Phys. Rev. A **29**, 1709 (1984).

[89] J. M. Ajello (private communication).
[90] K. P. Huber and C. Jungen, J. Chem. Phys. **92**, 850 (1990).
[91] A. N. Heays, Ph.D. thesis, The Australian National University, 2010.
[92] J. M. Ajello, G. K. James, and M. Ciocca, J. Phys. B **31**, 2437 (1998).
[93] X. M. Liu, D. E. Shemansky, M. Ciocca, I. Kanik, and J. M. Ajello, Astrophys. J. **623**, 579 (2005).
[94] J. Bishop, M. H. Stevens, and P. D. Feldman, J. Geophys. Res., [Space Phys.] **112**, A10312 (2007).
[95] J. S. Allen and C. C. Lin, Phys. Rev. A **39**, 383 (1989).
[96] D. E. Shemansky, I. Kanik, and J. M. Ajello, Astrophys. J. **452**, 480 (1995).
[97] J. F. M. Aarts and F. J. de Heer, Physica **52**, 45 (1971).
[98] R. S. Mangina, J. M. Ajello, R. A. West, and D. Dziczek, Astrophys. J. Suppl. Ser. **196**, 13 (2011).
[99] K. Becker, J. L. Forand, P. W. Zetner, and J. W. McConkey, J. Phys. B **17**, L915 (1984).
[100] J. C. Huschilt, H. W. Dassen, and J. W. McConkey, Can. J. Phys. **59**, 1893 (1981).
[101] A. R. Filippelli, C. C. Lin, L. W. Anderson, and J. W. McConkey, Adv. At., Mol., Opt. Phys. **33**, 1 (1994).
[102] R. S. Freund, J. Chem. Phys. **54**, 1407 (1971).